1971

Radiant interchange in a non-isothermal rectangular cavity

Tilak Raj Sawheny

RADIANT INTERCHANGE IN A NON-ISOTHERMAL RECTANGULAR CAVITY

BY

TILAK RAJ SAWHENY, 1946-

A THESIS

Presented to the Faculty of the Graduate School of the

UNIVERSITY OF MISSOURI-ROLLA

In Partial Fulfillment of the Requirements for the Degree

MASTER OF SCIENCE IN MECHANICAL ENGINEERING

1971

Approved by

A. L. Crosbie (Advisor) D. C. Look

H. H. Sieheltan Jr.

Dedicated to

my grand parents

Mr. and Mrs. Ishwar Dass Sawheny

ABSTRACT

Radiant interchange between non-isothermal, gray diffuse surfaces with non-uniform radiosity has been determined for a rectangular cavity. Temperature distribution and heat flux as thermal specifications for the parallel surfaces of the cavity have been considered separately. Ambarzumian's method has been used for the first time to solve a radiant interchange problem. According to the method, the integral equation for the radiosity is first transformed into an integro-differential equation and then into a system of ordinary differential equations. Initial conditions required to solve the differential equations are the H-functions. The H-functions represent the radiosity at the edge of the cavity for various temperature profiles. Applying Ambarzumian's method a closed-form expression for radiosity and heat transfer are obtained in terms of universal functions. Heat transfer from the cavity can be determined without knowing the radiosity inside the cavity. The numerical results for the H-functions, radiosity, local heat flux, overall heat transfer, local and overall apparent emittance for the cavity have been presented in the form of tables and graphs.

ACKNOWLEDGEMENTS

The author is grateful to Dr. Alfred L. Crosbie, for suggestion of the thesis topic, continuous guidance, encouragement and valuable suggestions throughout the course of this work. The author expresses his gratitude to Dr. D.C. Look for his critical review of the work and for the financial help under student assistance.

Thanks to Mrs. Carol Rodman for typing the thesis.

TABLE OF CONTENTS

LIST OF FIGURES

List of Figures (continued) Page

LIST OF TABLES

NOMENCLATURE

Symbol	Significance
A_j	Area of a surface j of the cavity
B	Dimensionless radiosity defined by equation (3-8)
$\overline{B}$	Laplace transform of dimensionless radiosity defined by equation (3-30)
B^+	Radiosity defined by equation (3-1)
B^*	Dimensionless radiosity defined by equation (3-7)
F	Numerical quadrature used in equation (4-5)
f	Kernel for the integral equation (4-1)
G	Irradiation
H	H-function
h	Distance between the parallel surfaces of the cavity
J_1	Bessel Function of first order
K	Kernel defined by equation (3-6)
m	Temperature distribution parameter
N	Number of quadrature points
Q	Heat transfer of the cavity defined by equation (3-16)
Q^*	Overall heat transfer of the cavity defined by equation (3-15)
Q_ϕ	Heat transfer of the cavity defined by equation (3-17)
q	Local heat flux defined by equation (3-12)

q^*	Local heat flux defined by equation (3-10)
q_ϕ	Local heat flux defined by equation (3-13)
q_0	Specified heat flux in section E.
r_i	Roots of Bessel Function of first order
S	Longman's numerical quadrature defined by equation (4-16)
s	Variable used in Laplace-transform
T_0	Temperature specified
T_r	Reference temperature
T_b	Temperature of the black surface
V_N	Terms in Euler's transformation shown in equation (4-7)
X	Depth into cavity
x	Dimensionless depth into the cavity
Y	Co-ordinate axis perpendicular to the plane of the paper
Z	Axis in vertical direction

Greek Symbols

α_0	Zeroth moment of H-function
α_1	First moment of H-function
ε	Emittance of the surface
σ	Stefan-Boltzmann Constant
ϕ	Dimensionless radiosity defined by equation (3-9)
ρ	Reflectance of the surface
ε_a	Apparent emittance of the cavity
$\bar{\varepsilon}_a$	Overall apparent emittance of the cavity

I. INTRODUCTION

New interest in radiative heat transfer has been stimulated in the past few years by the applications in new technologies. Specific examples of the applications include space-vehicle environmental control, solar energy conversion devices, power plants for space exploration, propulsion systems, furnaces, cavities, etc. Radiant interchange between surfaces is an important consideration in the examples mentioned above. In space, convection is absent and radiation is the only means by which waste heat from power plants, electronic equipment and other sources can be removed. Cavities are often used for thermal sources. Radiative interchange within the cavities is the fundamental criterion of their performance.

Many investigators have attempted to solve problems concerning radiant interchange between surfaces with different configurations and thermal specifications. Reviewing the investigations made in the past reveals that most of the work done involves gray diffuse isothermal surfaces with uniform radiosity. The investigators who considered the realistic case of non-uniform radiosity had to overcome the hurdle of solving an integral equation for the radiosity. Only for two special cases [(i) Spherical cavities and (ii) Circular arc cavity] have the integral equations been solved in closed form. For the other cases investigated, the integral equations were solved either by an approximate analytical method or by a numerical technique.

The present investigation deals with a subject which has received little attention in the past. It concerns the radiant interchange between gray, diffuse, non-isothermal surfaces with non-uniform radiosity. As compared with the work done on isothermal surfaces, the non-isothermal analysis seems more realistic. In the present study the temperature is assumed to decay exponentially with the depth into the cavity. The temperature distribution is varied by changing the damping co-efficient, and for each temperature distribution, there is an integral equation to be solved.

The approach taken to tackle the present problem has been used in gaseous radiation studies and is known as Ambarzumian's method. The method is applied for the first time to determine radiant interchange between surfaces. According to the method the integral equation for the radiosity is transformed into integro-differential equation which is then represented by a system of differential equations. The H-function defined as the radiosity at the edge of the cavity represents the initial conditions for solving the system of the differential equations. The H-function is determined by numerically solving a nonlinear Fredholm integral equation of second kind.

Applying Ambarzumian's method an analysis for the determination of radiant interchange between the non-isothermal surfaces of the rectangular cavity is presented in Chapter III. Closed-form expressions for the radiosity and heat transfer for various temperature profiles are achieved from the analysis in terms of universal functions. Utilizing the closed-form relations, the heat transfer from the cavity can be computed without knowing the radiosity inside the cavity. A digital computer is employed to obtain the numerical results for the H-functions and radiosity. Numerical techniques and results are presented in Chapter IV. Conclusions of the present investigation along with recommendations for further study are given in Chapter V.

II. REVIEW OF LITERATURE

Radiant interchange between surfaces is one of the fundamental and important problems in the field of radiative heat transfer. A lot of work has been done involving various configurations with different physical and thermal conditions. The present review is restricted to the literature concerning radiant interchange between gray diffuse surfaces with non-uniform radiosity. The space between the surfaces is filled with a non-participating media.

Past studies are presented in chronological order in Table 2.1. Geometry, physical and thermal conditions specified and the method used to solve the problem have been listed in this table. The geometries considered in past investigations are shown in Figure 2.1. By reviewing the literature presented in the table, one finds that most of the work concerns geometries 1 and 3. The investigations dealing with these geometries are in references [6,8,12,13,15,16,17,19,20] and [8,16,18,19] respectively. The study of the cylindrical cavities are mentioned in references [1,2,7] for geometry 4 and in references [3,5, 14] for geometry 5. Few investigators have worked on the problems involving finite, non-parallel surfaces, tapered tubes and conical cavities as mentioned in the Table 2.1. Geometry 4 with heat flux specification to the surfaces has been considered in reference [7]. A problem involving non-isothermal surfaces for geometry 11 without any opening has been investigated in reference [4]. The rest of the research has been conducted for isothermal surfaces.

Every problem presented in the Table 2.1 involves an integral equation for the non-uniform radiosity. Exact solutions have not yet been achieved except for radiant transfer in (a) Spherical cavities (geometry 11), reference [10] and (b) Cylindrical arc cavity (geometry 12), reference [21]. Besides the two closed-form solutions, the methods used in rest of the work to solve the radiosity equations are listed as follows:

A. Approximate Kernel Method [1,2,7]

B. Asymptotic Behavior [18]

C. Least Square Method [20]

D. Sokolv's Method [15,16]

E. Successive Iteration Method [5,7,8,9,19]

F. Variational Method [6,7,12]

G. Zonal Method [11,14]

The approximate methods used by the investigators involve simple mathematics. The survey made may be incomplete, but it seems that little interest has been shown to radiant interchange between non-isothermal surfaces. The present study refers to non-isothermal surfaces with non-uniform radiosity. Geometry 10 is selected as the configuration of interest. In this work, the emphasis is placed upon getting a closed-form solution for the radiosity and the heat transfer in terms of standard universal functions. Application of Ambarzumian's method is employed to achieve this goal.

Table 2.1

Review of Literature Table

Year	Reference	Geometry	Physical situation	Method of solution
		Description of the problem		
1927 1928	Buckley [1,2]	4	Isothermal surfaces	Approximate Kernel Method
1935	Eckert [3]	5	Isothermal surfaces	Approximate Radiosity By Straight Lines Segments
1936	Moon [4]	11	Non-isothermal surfaces	Closed-Form Solution
1960	Sparrow and Albers [5]	5	Isothermal walls	Iterative Technique
1960	Sparrow [6]	1	Isothermal surfaces	Variational Method
1960	Usisken and Seigel [7]	4	Specified wall heat flux. Black and gray radiation analyses.	Approximate Kernel Method, Iterative, Variational Method
1961	Sparrow, Gregg, Szel, Manos [8]	1,3	Gray, isothermal surfaces	Iterative Technique
1961	Sparrow and Gregg [9]	7	Isothermal surfaces	Iterative Technique
1962	Sparrow and Jonsson [10]	11	Isothermal surfaces	Closed-Form Solution
1964	Sparrow and Jonsson [11]	2,6	Isothermal and adiabatic surfaces	Zonal Method (Angle Factor Algebra)
1965	Sparrow and Sheikh [12]	1	Isothermal surfaces	Generalized Variational Method
1966	Love and Gilbert [13]	1	Isothermal surfaces	Experimental
1967	Campanaro and Ricolfi [14]	5,8	Isothermal surfaces	Zonal Method

Table 2.1 (continued)

Year	Reference	Geometry	Physical situation	Method of solution
1967	Crosbie and Viskanta [15]	1	Isothermal surfaces	Sokolv's Method
1968	Love and Turner [16]	1,3	Isothermal surfaces	Sokolv's Method
1969	Toor, Viskanta, and Winter [17]	1,9	Specular and diffuse isothermal surfaces	Monte Carlo Method and Experimental
1970	Rasmussen and Jischke [18]	3	Isothermal surfaces	Asymptotic Behavior
1970	Look and Love [19]	1,3	Isothermal surfaces	Iterative Technique
1970	Sparrow and Sheikh [20]	1	Isothermal surfaces	Least Squares Method
1970	Sparrow and Cess [21]	11,12	Isothermal surfaces	Closed-Form Solution

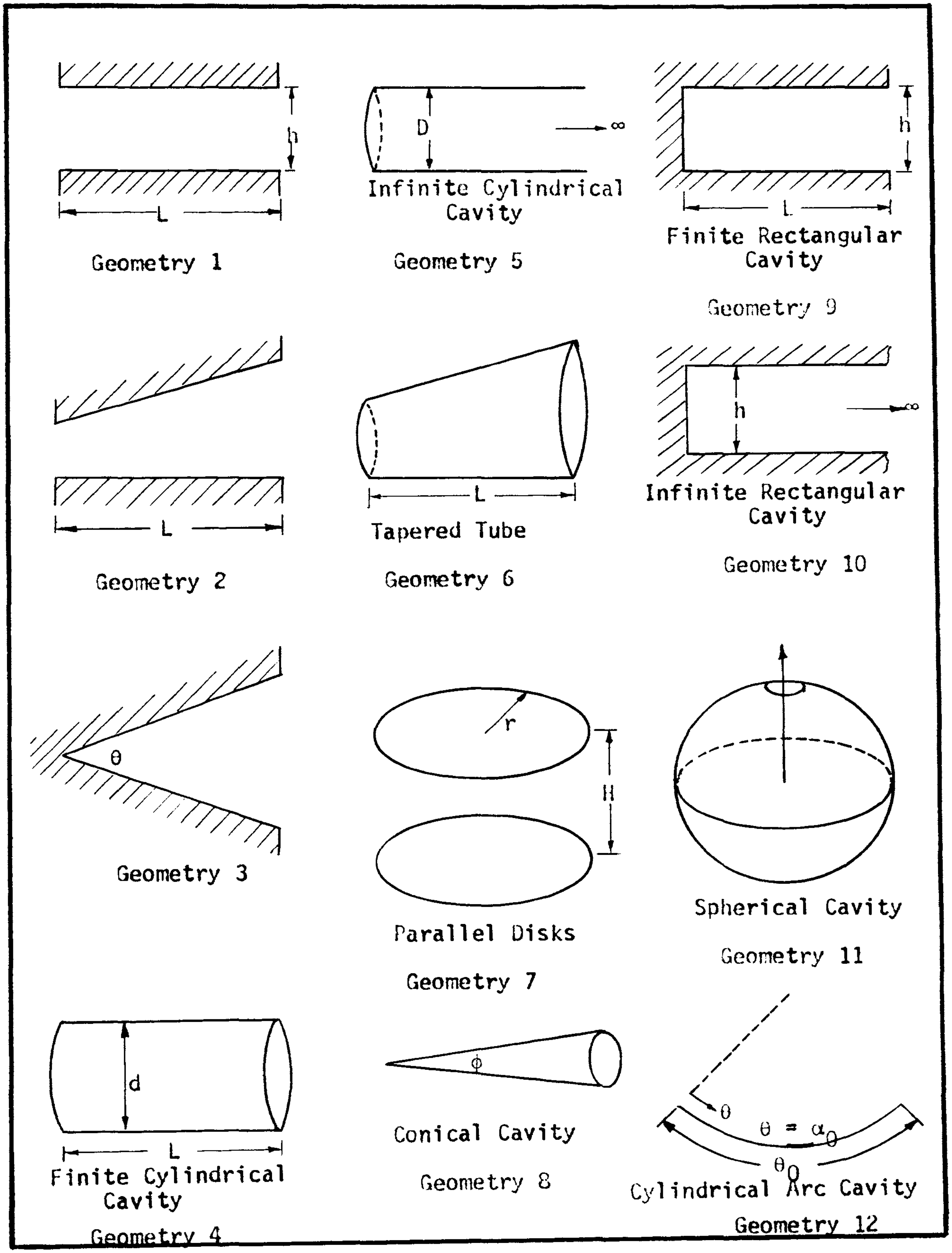

Figure 2.1 - Figures illustrating different geometries

III. ANALYSIS

A. PHYSICAL MODEL AND GOVERNING EQUATIONS

The present study deals with the configuration shown in Figure 3.1. Surfaces one and two extend indefinitely into and out of the plane of the paper. Assumptions made for the analysis are given as follows:

(i) Surfaces one and two are gray and diffuse with non-uniform radiosity.

(ii) Surfaces one and two have the same properties, i.e., $\varepsilon_1 = \varepsilon_2 = \varepsilon$; $\rho_1 = \rho_2 = \rho$.

(iii) There is no participating medium between the surfaces.

(iv) Surface three is black and isothermal at a temperature T_b.

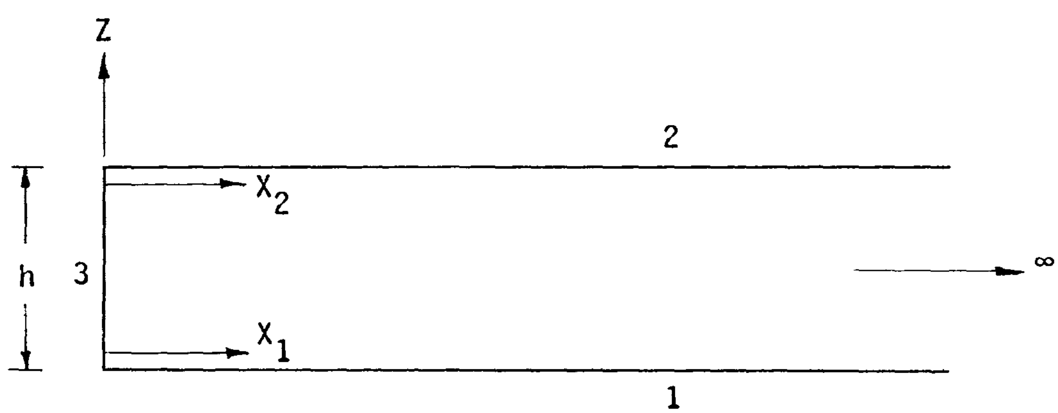

Figure 3.1 - Rectangular cavity

The temperature distributions for surfaces one and two ($T_0(X_1)$ and $T_0(X_2)$) are identical to each other. Because of the symmetry of the configuration only one surface is considered in the analysis. The radiosity of surface one can be expressed in general as

$$B^+(X_1) = \varepsilon\sigma T_0^{\ 4}(X_1) + \rho G(X_1) \quad . \tag{3-1}$$

The first term on the right side of equation (3-1) represents the radiant flux being emitted by surface one from location X_1, and $G(X_1)$ is the irradiation at location X_1 from the other surfaces to surface one. The radiosity equation (3-1) can be re-written as follows [22]

$$\begin{aligned} B^+(X_1) = \varepsilon\sigma T_0^{\ 4}(X_1) &+ \rho\iint_{A_3} B^+(Z)\,\frac{\cos\theta_1\cdot\cos\theta_3}{\pi R_{13}^2}\,dA_3 \\ &+ \rho\iint_{A_2} B^+(X_2)\,\frac{\cos\theta_1\cdot\cos\theta_2}{\pi R_{12}^2}\,dA_2 \end{aligned} \tag{3-2}$$

where

$$\cos\theta_1 = \cos\theta_2 = h/R_{12} \quad , \quad R_{12}^2 = (X_1-X_2)^2 + (Y_1-Y_2)^2 + h^2 \ ;$$

$$\cos\theta_3 = X_1/R_{13} \quad , \quad R_{13}^2 = X_1^{\ 2} + (Y_1-Y_3)^2 + Z^2 \quad .$$

Now equation (3-2) can be written as

$$\begin{aligned} B^+(X_1) = \varepsilon\sigma T_0^{\ 4}(X_1) &+ \rho\int_0^h\int_{-\infty}^{\infty} \frac{B^+(Z)h^2dZdY_3}{\pi[X_1^2+(Y_1-Y_3)^2+Z^2]^2} \\ &+ \rho\int_0^{\infty}\int_{-\infty}^{\infty} \frac{B^+(X_2)h^2dX_2dY_2}{\pi[(X_1-X_2)^2+(Y_1-Y_2)^2+h^2]^2} \end{aligned} \tag{3-3}$$

where Y_1, Y_2, Y_3 represent the coordinate axes perpendicular to the plane of the paper for the surfaces one, two and three, respectively.

After integrating, equation (3-3) becomes

$$B^+(X_1) = \varepsilon\sigma T_0{}^4(X_1) + \frac{\rho}{2}\sigma T_b{}^4\left[1 - \frac{X_1}{\sqrt{X_1{}^2+h^2}}\right] + \frac{\rho}{2}\int_0^\infty \frac{B^+(X_2)h^2dX_2}{[(X_1-X_2)^2+h^2]^{3/2}} \,. \qquad 3\text{-}4$$

Introducing $x = X_1/h$ and $y = X_2/h$, and assuming the temperature decays exponentially, i.e., $T_0(x) = T_r \exp(-mx/4)$, the integral equation for the radiosity (3-4) takes the form

$$B^*(x,m) = \varepsilon\sigma T_r{}^4 e^{-mx} + \frac{\rho}{2}\sigma T_b{}^4\left[1 - \frac{x}{\sqrt{x^2+1}}\right] + \frac{\rho}{2}\int_0^\infty B^*(y,m)K(|x-y|)dy \qquad 3\text{-}5$$

where the kernel is defined as

$$K(|x-y|) = K(x,y) = \frac{1}{[(x-y)^2+1]^{3/2}} \,. \qquad 3\text{-}6$$

The emissive power decays much faster than the temperature. Since integral equation (3-5) is linear, $B^*(x,m)$ can be expressed as the superposition of two functions

$$B^*(x,m) = \varepsilon\sigma T_r{}^4 B(x,m) + \rho\sigma T_b{}^4\phi(x) \qquad 3\text{-}7$$

where $B(x,m)$ and $\phi(x)$ satisfy the following two integral equations

$$B(x,m) = e^{-mx} + \frac{\rho}{2}\int_0^\infty B(y,m)K(|x-y|)dy \qquad 3\text{-}8$$

and

$$\phi(x) = \frac{1}{2}\left[1 - \frac{x}{\sqrt{x^2+1}}\right] + \frac{\rho}{2}\int_0^\infty \phi(y)K(|x-y|)dy \,. \qquad 3\text{-}9$$

Physically, $B(x,m)$ is the dimensionless radiosity for the case when the temperature of black surface three is zero. And $\phi(x)$ represents the dimensionless radiosity $(B^*/\rho\sigma T_b{}^4)$ for the case when the temperature of surfaces one and two is zero.

The local heat flux can be written as

$$q^*(x,m) = \frac{\varepsilon}{\rho}\left[\sigma T_r^{\,4}\ e^{-mx} - B^*(x,m)\right] . \qquad \text{3-10}$$

Using expression (3-8), the local heat flux can be expressed as

$$q^*(x,m) = \varepsilon\sigma T_r^{\,4} q(x,m) - \varepsilon\sigma T_b^{\,4} q_\phi(x) \qquad \text{3-11}$$

where

$$q(x,m) = \frac{1}{\rho}\,[e^{-mx} - \varepsilon B(x,m)] \qquad \text{3-12}$$

and

$$q_\phi(x) = \phi(x) . \qquad \text{3-13}$$

The overall heat transfer per unit length of cavity is

$$Q^* = 2h\int_0^\infty q^*(x,m)dx \qquad \text{3-14}$$

or

$$Q^* = 2h\varepsilon\sigma T_r^{\,4} Q(m) - 2h\varepsilon\sigma T_b^{\,4} Q_\phi \qquad \text{3-15}$$

where

$$Q(m) = \int_0^\infty q(x,m)dx = \frac{1}{\rho}\int_0^\infty \left[e^{-mx} - \varepsilon B(x,m)\right] dx \qquad \text{3-16}$$

and

$$Q_\phi = \int_0^\infty q_\phi(x)dx = \int_0^\infty \phi(x)dx \qquad \text{3-17}$$

$Q(m)$ is the heat transfer from the cavity when the surface three is held at 0°R. $Q(m)$ depends on the temperature distribution parameter m and the reflectance ρ. Q_ϕ is the heat transfer to the cavity from the black surface three when surfaces one and two are held at 0°R.

The analysis of $B(x,m)$, $\phi(x)$, $Q(m)$ and Q_ϕ are carried out in detail in this chapter.

B. DIMENSIONLESS RADIOSITY, $B(x,m)$.

The equation (3-8) for the dimensionless radiosity $B(x,m)$ is classified as a linear Fredholm integral equation of second kind. $B(x,m)$ depends on the depth into the cavity x, the reflectance ρ and the temperature distribution m. In this section Ambarzumian's method [23] transforms the integral equation into an integro-differential equation. The dimensionless radiosity $B(o,m)$ at the edge of the cavity, the H-function, is the initial condition for the integro-differential equation. A nonlinear Fredholm integral equation for the H-function is developed.

1. INTEGRO-DIFFERENTIAL EQUATION.

The equation (3-8) for dimensionless radiosity $B(x,m)$ can be re-written as follows

$$B(x,m) = e^{-mx} + \frac{\rho}{2}\int_0^x B(y,m)K(x-y)dy + \frac{\rho}{2}\int_x^\infty B(y,m)K(y-x)dy \quad . \quad 3\text{-}18$$

Substituting $z = x-y$ in the first integral and $z = y-x$ in the second integral of the right hand side of equation (3-18) yields

$$B(x,m) = e^{-mx} + \frac{\rho}{2}\int_0^x B(x-z,m)K(z)dz + \frac{\rho}{2}\int_0^\infty B(x+z,m)K(z)dz \quad . \qquad 3\text{-}19$$

Differentiating equation (3-19) with respect to x gives

$$\frac{\partial B(x,m)}{\partial x} = -me^{-mx} + \frac{\rho}{2} B(o,m)K(x) + \frac{\rho}{2}\int_0^x \frac{\partial B(x-z,m)}{\partial x} K(z)dz$$

$$+ \frac{\rho}{2}\int_0^\infty \frac{\partial B(x+z,m)}{\partial x} K(z)dz \quad . \qquad 3\text{-}20$$

Now substituting $y = x-z$ in the first integral and $y = x+z$ in the second integral of the right hand side of equation (3-20) yields the following integral equation for the derivative of $B(x,m)$

$$\frac{\partial B(x,m)}{\partial x} = - me^{-mx} + \frac{\rho}{2} B(o,m)K(x) + \frac{\rho}{2}\int_0^\infty \frac{\partial B(y,m)}{\partial x} K(|x-y|)dy \qquad 3\text{-}21$$

or

$$\frac{\partial B(x,m)}{\partial x} = - me^{-mx} + \frac{\rho}{2} B(o,m)\int_0^\infty te^{-xt}J_1(t)dt$$

$$+ \frac{\rho}{2}\int_0^\infty \frac{\partial B(y,m)}{\partial x} K(|x-y|)dy \qquad 3\text{-}22$$

where

$$K(x) = \int_0^\infty te^{-xt}J_1(t)dt \quad . \qquad 3\text{-}23$$

represents the Laplace's transform of $tJ_1(t)$.

The solution of equation (3-21) is determined by method of superposition. Multiplying equation (3-8) by

$$\frac{\rho}{2} mJ_1(m)dm$$

and then integrating from 0 to ∞ yields

$$\frac{\rho}{2}\int_0^\infty mB(x,m)J_1(m)dm = \frac{\rho}{2}K(x) + \frac{\rho}{2}\int_0^\infty m\left[\frac{\rho}{2}\int_0^\infty B(y,m)K(|x-y|)dy\right]J_1(m)dm \; . \qquad 3\text{-}24$$

Multiplying equation (3-8) by -m and equation (3-24) by B(o,m) and adding gives

$$\left[- mB(x,m) + \frac{\rho}{2}B(o,m)\int_0^\infty mB(x,m)J_1(m)dm\right]$$

$$= - me^{-mx} + \frac{\rho}{2}B(o,m)K(x)$$

$$+ \frac{\rho}{2}\int_0^\infty\left[- mB(y,m) + \frac{\rho}{2}B(o,m)\int_0^\infty mJ_1(m)B(y,m)dm\right]K(|x-y|)dy \; . \qquad 3\text{-}25$$

Comparing equations (3-21) and (3-25), the solution to equation (3-21) is

$$\frac{\partial B(x,m)}{\partial x} = - mB(x,m) + \frac{\rho}{2}B(o,m)\int_0^\infty nB(x,n)J_1(n)dn \; . \qquad 3\text{-}26$$

Notice the radiosity equation (3-26) is an integro-differential equation instead of a linear Fredholm integral equation. The boundary condition B(o,m) is needed before this equation can be solved.

2. H-FUNCTION.

In physical sense, H-function is the radiosity at the edge of the cavity B(o,m). The aim of this section is to achieve a nonlinear integral equation for H-function which is convenient for numerical solution. Evaluating equation (3-8) at x = 0 yields

$$B(o,m) = 1 + \frac{\rho}{2}\int_0^\infty B(y,m)K(y)dy \qquad 3\text{-}27$$

or

$$B(o,m) = 1 + \frac{\rho}{2}\int_0^\infty B(y,m)\int_0^\infty te^{-yt}J_1(t)dt\ dy \qquad 3\text{-}28$$

where again

$$K(y) = \int_0^\infty te^{-yt}J_1(t)dt\ .$$

By changing the order of integration, equation (3-28) can be written as

$$B(o,m) = 1 + \frac{\rho}{2}\int_0^\infty nJ_1(n)\overline{B}(n,m)dn \qquad 3\text{-}29$$

where

$$\overline{B}(n,m) = L_n\{B(y,m)\} = \int_0^\infty B(y,m)e^{-ny}dy\ . \qquad 3\text{-}30$$

Thus $B(o,m)$ may be expressed in terms of Laplace transform of the dimensionless radiosity $B(y,m)$ and Bessel function of the first kind. $\overline{B}(n,m)$ can be expressed in terms of $B(o,m)$ by applying a Laplace transform to equation (3-26)

$$s\overline{B}(s,m) - B(o,m) = -\ m\overline{B}(s,m) + \frac{\rho}{2}B(o,m)\int_0^\infty \overline{B}(s,n)nJ_1(n)dn \qquad 3\text{-}31$$

or

$$(s+m)\overline{B}(s,m) = B(o,m)\left[1 + \frac{\rho}{2}\int_0^\infty n\overline{B}(s,n)J_1(n)dn\right]. \qquad 3\text{-}32$$

Compare equation (3-29) with the right hand side of equation (3-32). In order to replace the term of equation (3-32) in brackets by $B(o,s)$, $\overline{B}(s,n)$ must be symmetric.

The first step in showing $\overline{B}(s,n)$ symmetric is to rewrite equation (3-8) as

$$B(x,s) = e^{-sx} + \frac{\rho}{2}\int_0^\infty B(y,s)K(|x-y|)dy \qquad 3\text{-}33$$

and

$$B(x,n) = e^{-nx} + \frac{\rho}{2}\int_0^\infty B(y,n)K(|x-y|)dy \ . \qquad 3\text{-}34$$

Multiplying equation (3-33) and (3-34) respectively by $B(x,n)$ and $B(x,s)$ and integrating both with respect to x over the interval $(0,\infty)$ gives

$$\int_0^\infty B(x,s)\ B(x,n)dn = \int_0^\infty B(x,n)\left[\frac{\rho}{2}\int_0^\infty B(y,s)K(|x-y|)dy\right]dx + \int_0^\infty e^{-sx}B(x,n)dx \qquad 3\text{-}35$$

and

$$\int_0^\infty B(x,n)\ B(x,s)dx = \int_0^\infty B(x,s)\left[\frac{\rho}{2}\int_0^\infty B(y,n)K(|x-y|)dy\right]dx + \int_0^\infty e^{-nx}B(x,s)dx \ . \qquad 3\text{-}36$$

The left sides of the equations (3-35) and (3-36) are identical. Since the kernel $K(x,y)$ is symmetric, the first terms on the right side of the equations are identical. The last terms of (3-35) and (3-36) must therefore be equal

$$\int_0^\infty e^{-sx}B(x,n)dx = \int_0^\infty e^{-nx}B(x,s)dx \ . \qquad 3\text{-}37$$

Equation (3-37) can be rephrased as

$$\overline{B}(s,n) = \overline{B}(n,s) \ . \qquad 3\text{-}38$$

Therefore $\overline{B}(s,n)$ is symmetric.

Using equation (3-38), equation (3-29) can be written as

$$B(o,m) = 1 + \frac{\rho}{2}\int_0^\infty nJ_1(n)\overline{B}(m,n)dn \ . \qquad 3\text{-}39$$

Replacing n with s in equation (3-39) and substituting this equation into equation (3-32) yields

$$(s+m)\overline{B}(s,m) = B(o,m)B(o,s) \qquad 3\text{-}40$$

or

$$\overline{B}(s,m) = \frac{B(o,m)B(o,s)}{s+m} \qquad 3\text{-}41$$

Substitution of equation (3-41) into equation (3-39) gives

$$B(o,m) = 1 + \frac{\rho}{2}B(o,m)\int_0^\infty \frac{nJ_1(n)B(o,n)}{n+m}dn \ . \qquad 3\text{-}42$$

Utilizing the definition of the H-function, i.e., $H(m) = B(o,m)$, equation (3-42) becomes

$$H(m) = 1 + \frac{\rho}{2}H(m)\int_0^\infty \frac{nJ_1(n)H(n)}{n+m}dn \ . \qquad 3\text{-}43$$

Since equation (3-43) would converge very slowly on application of an iterative technique, another form of the equation is needed. Using

$$\frac{n}{n+m} = 1 - \frac{m}{n+m} \ ,$$

equation (3-43) becomes

$$H(m) = 1 + \frac{\rho}{2} H(m) \int_0^\infty J_1(n)H(n)dn - \frac{\rho}{2} H(m) \int_0^\infty \frac{mJ_1(n)H(n)}{n+m} dn \ . \qquad 3\text{-}44$$

Dividing the equation (3-44) by H(m) yields

$$\frac{1}{H(m)} = 1 - \frac{\rho}{2}\alpha_0 + \frac{\rho}{2}\int_0^\infty \frac{mJ_1(n)H(n)}{n+m} dn \qquad 3\text{-}45$$

where α_0 is the zeroth moment of the H-function

$$\alpha_0 = \int_0^\infty H(n)J_1(n)dn \ . \qquad 3\text{-}46$$

α_0 can be determined by multiplying equation (3-43) by $J_1(m)dm$ and integrating over the interval $(0,\infty)$, thus

$$\alpha_0 = \int_0^\infty H(m)J_1(m)dm = \int_0^\infty J_1(m)dm + \frac{\rho}{2}\int_0^\infty\int_0^\infty \frac{nH(m)J_1(m)H(n)J_1(n)}{n+m} dn\ dm \ . \qquad 3\text{-}47$$

Since m and n are dummy variables, in the second integral of the extreme right hand side of equation (3-47) these variables may be interchanged yielding

$$\int_0^\infty H(m)J_1(m)dm = \int_0^\infty J_1(m)dm + \frac{\rho}{2}\int_0^\infty\int_0^\infty \frac{mH(n)J_1(n)H(m)J_1(m)}{m+n} dm\ dn \ . \qquad 3\text{-}48$$

The expression obtained by adding equations (3-47) and (3-48) is

$$2\int_0^\infty H(m)J_1(m)dm = 2\int_0^\infty J_1(m)dm + \frac{\rho}{2}\int_0^\infty\int_0^\infty H(m)J_1(m)\ H(n)J_1(n)\ dm\ dn \ . \qquad 3\text{-}49$$

Using the definition of α_0, equation (3-49) can be reduced to a quadratic equation of the form

$$\rho\alpha_0^{\,2} - 4\alpha_0 + 4 = 0 \; . \qquad 3\text{-}50$$

The solutions of equation (3-50) are

$$\alpha_0^{\,+} = \frac{2}{\rho}\,[1 + \sqrt{1-\rho}]$$

$$\qquad\qquad 3\text{-}51$$

$$\alpha_0^{\,-} = \frac{2}{\rho}\,[1 - \sqrt{1-\rho}]$$

Only the substitution of $\alpha_0^{\,-}$ into equation (3-45) gives meaningful expression for the H-function

$$\frac{1}{H(m)} = \sqrt{1-\rho} + \frac{\rho}{2}\int_0^\infty \frac{mJ_1(n)H(n)}{n+m}\,dn \; . \qquad 3\text{-}52$$

For m = 0, equation (3-52) yields

$$H(0) = B(0,0) = \frac{1}{\sqrt{1-\rho}} = \frac{1}{\sqrt{\varepsilon}} \; . \qquad 3\text{-}53$$

From the above equation, the equation the dimensionless radiosity at the edge of an isothermal cavity is equal to the inverse of the square root of the emittance.

Thus equations (3-52) and (3-26) can be solved for the H-function and radiosity respectively. Numerical solution techniques for these equations are presented in the next chapter.

C. DIMENSIONLESS RADIOSITY, $\phi(x)$.

Equation (3-9) for the dimensionless radiosity, $\phi(x)$, falls into the category of a linear Fredholm integral equation of the second kind. $\phi(x)$ depends upon the depth in the cavity x and the reflectance ρ. An expression for $\phi(x)$ in terms of the dimensionless radiosity $B(x,m)$ along with the development of a differential equation for $\phi(x)$ is presented in this section.

The Laplace transform of $J_1(m)$ can be expressed as

$$\int_0^\infty e^{-xm} J_1(m)dm = 1 - \frac{x}{\sqrt{x^2+1}} . \qquad 3\text{-}54$$

Using equation (3-54), equation (3-9) becomes

$$\phi(x) = \frac{1}{2}\int_0^\infty e^{-mx} J_1(m)dm + \frac{\rho}{2}\int_0^\infty \phi(y)K(|x-y|)dy . \qquad 3\text{-}55$$

Multiplying equation (3-8) by

$$\frac{1}{2} J_1(m)dm$$

and integrating over the interval $(0,\infty)$ yields

$$\frac{1}{2}\int_0^\infty J_1(m)B(x,m)dm = \frac{1}{2}\int_0^\infty e^{-mx}J_1(m)dm$$

$$+ \int_0^\infty \frac{\rho}{2}\int_0^\infty \frac{1}{2} J_1(m)B(y,m)K(|x-y|)dydm . \qquad 3\text{-}56$$

Comparing equations (3-55) and (3-56) gives

$$\phi(x) = \frac{1}{2}\int_0^\infty J_1(m)B(x,m)dm . \qquad 3\text{-}57$$

Since a differential equation is easier to solve than an integral equation, equation (3-9) is transformed into a differential equation for $\phi(x)$. Multiplying equation (3-26) by $J_1(m)dm$ and integrating over the interval $(0,\infty)$ yields

$$\int_0^\infty \frac{J_1(m)\partial B(x,m)}{\partial x} dm = - \int_0^\infty mJ_1(m)B(x,m)dm$$

$$+ \frac{\rho}{2}\int_0^\infty J_1(m)B(o,m) \int_0^\infty nB(x,n)J_1(n)dndm \qquad 3\text{-}58$$

or

$$\frac{\partial}{\partial x}\int_0^\infty J_1(m)B(x,m)dm = -\int_0^\infty mJ_1(m)B(x,m)dm$$

$$+\frac{\rho}{2}\int_0^\infty J_1(m)H(m)dm\int_0^\infty nB(x,n)J_1(n)dn \; . \qquad 3\text{-}59$$

Using equations (3-46) and (3-57), the above equation can be written as

$$\frac{\partial\phi(x)}{\partial x} = -\frac{1}{2}\phi(x) + \frac{\rho}{4}\alpha_0\phi(x) \qquad 3\text{-}60$$

where

$$\phi(x) = \int_0^\infty mB(x,m)J_1(m)dm \; . \qquad 3\text{-}61$$

The initial condition for equation (3-60) is

$$\phi(0) = \frac{1}{2}\alpha_0 \; .$$

Differential equation (3-60) is solved in manner similar to equation (3-26). The details of the solution are given in the next chapter.

D. OVERALL DIMENSIONLESS HEAT TRANSFER, Q*.

The heat transfer from the rectangular cavity can be found from equation (3-15). The overall heat transfer from the cavity, Q*, is presented in terms of two dimensionless functions Q(m) and Q_φ in terms of the H-function and the moments of the H-function.

1. DIMENSIONLESS HEAT TRANSFER, Q(m).

Physically Q(m) is the overall dimensionless heat transfer from the cavity for the case when the temperature of the black surface three is zero. Referring back to the definition of Q(m), equation (3-16)

$$Q(m) = \frac{1}{\rho}\int_0^\infty [e^{-mx} - \varepsilon B(x,m)]\, dx \quad .$$

Using the expression for the radiosity, B(x,m), from equation (3-8), with the kernel

$$K(x,y) = \frac{1}{[(x-y)^2+1]^{3/2}} \;,$$

equation (3-16) yields

$$Q(m) = \frac{1}{\rho}\int_0^\infty \left[e^{-mx} - \varepsilon\left[e^{-mx} + \frac{\rho}{2}\int_0^\infty \frac{B(y,m)dy}{[(x-y)^2+1]^{3/2}} \right]\right] dx \;. \qquad \text{3-62}$$

After simplification the above equation becomes

$$Q(m) = \int_0^\infty e^{-mx}dx - \frac{\varepsilon}{2}\int_0^\infty B(y,m)\left[\int_0^\infty \frac{dx}{[(x-y)^2+1]^{3/2}}\right] dy \;. \qquad \text{3-63}$$

Evaluating the integral in parentheses in the last term of equation (3-63) gives

$$\int_0^\infty \frac{dx}{[(x-y)^2+1]^{3/2}} = 1 + \frac{y}{y^2+1} \quad . \qquad \text{3-64}$$

This relation can be expressed in terms of the Laplace transform of $J_1(t)$ as

$$1 + \frac{y}{y^2+1} = 2 - \int_0^\infty e^{-yt} J_1(t)dt \; . \qquad 3\text{-}65$$

Substituting equation (3-65) into equation (3-62) yields

$$Q(m) = \int_0^\infty e^{-mx}dx - \frac{\varepsilon}{2}\int_0^\infty B(y,m)\left[2 - \int_0^\infty e^{-yt}J_1(t)dt\right] dy \qquad 3\text{-}66$$

or

$$Q(m) = \int_0^\infty \left[e^{-mx} - \varepsilon B(x,m)\right] dx + \frac{\varepsilon}{2}\int_0^\infty J_1(t)\int_0^\infty e^{-yt}B(y,m)dy\ dt \; . \qquad 3\text{-}67$$

The first term of right side of equation (3-67) is $\rho Q(m)$. Using equation (3-41) with the definition of the H-function, equation (3-67) can be expressed as

$$Q(m) = \rho Q(m) + \frac{\varepsilon}{2}\int_0^\infty J_1(t)\ \frac{H(m)H(t)}{t+m}\ dt \; . \qquad 3\text{-}68$$

After simplification equation (3-68) may be reduced to

$$Q(m) = \frac{H(m)}{2}\int_0^\infty \frac{J_1(t)H(t)}{t+m}\ dt \; . \qquad 3\text{-}69$$

Equation (3-52) can be rephrased as

$$\frac{\rho m}{2}\int_0^\infty \frac{J_1(t)H(t)}{t+m}\ dt = \frac{1}{H(m)} - \sqrt{\varepsilon} \; . \qquad 3\text{-}70$$

Using equation (3-70), equation (3-69) becomes

$$Q(m) = \frac{1 - H(m)\sqrt{\varepsilon}}{\rho m} \; . \qquad 3\text{-}71$$

When surfaces one and two of the cavity are isothermal, $m = 0$, the dimensionless heat transfer from equation (3-69) can be expressed as

$$Q(o) = \frac{\alpha_1}{2\sqrt{\varepsilon}} \qquad 3\text{-}72$$

where α_1 is the first moment of the H-function

$$\alpha_1 = \int_0^\infty \frac{J_1(t)H(t)}{t}\,dt \; . \qquad 3\text{-}73$$

2. DIMENSIONLESS HEAT TRANSFER, Q_ϕ.

Q_ϕ represents the overall dimensionless heat transfer from the cavity for the case when the temperatures of surfaces one and two are zero. Using expression (3-57) for $\phi(x)$, equation (3-17) gives

$$Q_\phi = \frac{1}{2}\int_0^\infty \int_0^\infty J_1(m)B(x,m)dm\,dx \qquad 3\text{-}74$$

Equation (3-16) can be integrated, yielding

$$\int_0^\infty B(x,m)dx = \frac{\rho}{\varepsilon}\left[\frac{1}{\rho m} - Q(m)\right] \; . \qquad 3\text{-}75$$

Replacing Q(m) by expression (3-71), equation (3-75) reduces to

$$\int_0^\infty B(x,m)dx = \frac{H(m)}{\sqrt{\varepsilon}} \qquad 3\text{-}76$$

Substituting equation (3-76) into equation (3-74) yields

$$Q_\phi = \frac{1}{2}\int_0^\infty \frac{J_1(m)H(m)}{m\sqrt{\varepsilon}}\,dm = \frac{\alpha_1}{2\sqrt{\varepsilon}} \; . \qquad 3\text{-}77$$

E. PRESCRIBED HEAT FLUX.

In this section the analysis is presented for surface one and two with heat flux specified instead of the temperature. The heat fluxes for surfaces one and two [$q(X_1)$ and $q(X_2)$] are identical to each other as shown in Figure 3.2. Assumptions made in section A still hold for the analysis in this section.

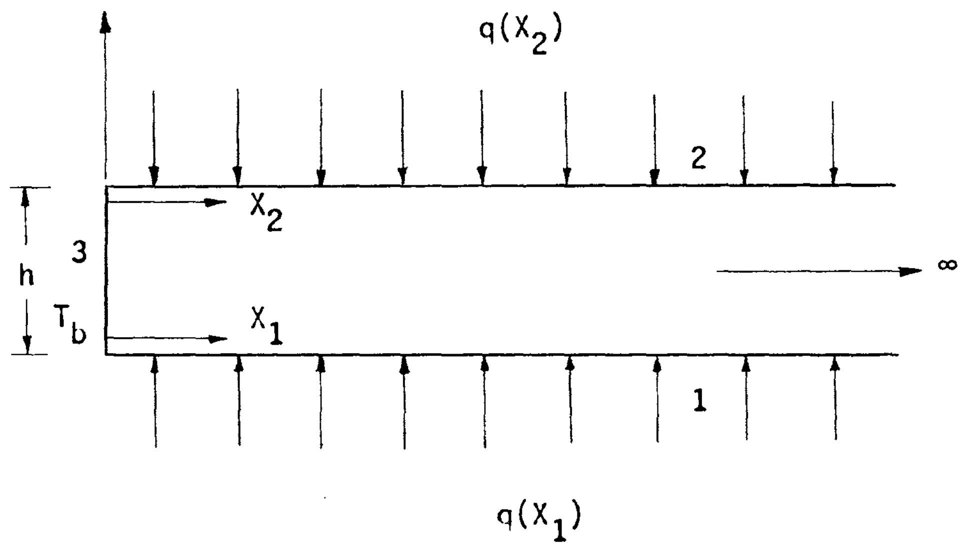

Figure 3.2 - Rectangular cavity with heat flux

Again because of symmetry of the configuration shown in Figure 3.2 surface one is considered for analysis for this section. The radiosity of surface one can be expressed in general as

$$B_f^+(X_1) = q(X_1) + G(X_1) \qquad 3\text{-}78$$

where $q(X_1)$ is the specified heat flux and $G(X_1)$ is irradiation from other surfaces at location X_1. Equation (3-78) can be rewritten as [22]

$$B_f^+(X_1) = q(X_1) + \iint_{A_3} \frac{B^+(Z)\cos\theta_1\ \cos\theta_3}{\pi R_{13}^2}\, dA_3$$

$$+ \iint_{A_2} \frac{B_f^+(X_2)\cos\theta_1\ \cos\theta_2}{\pi R_{12}^2}\, dA_2 \qquad 3\text{-}79$$

where $\cos\theta_1 = \cos\theta_2 = h/R_{12}$, $R_{12}^2 = (X_1-X_2)^2 + (Y_1-Y_2)^2 + h^2$;

$\cos\theta_3 = X_1/R_{13}$, $R_{13}^2 = X_1{}^2 + (Y_1-Y_3)^2 + Z^2$.

Now equation (3-79) becomes

$$B_f^+(X_1) = q(X_1) + \int_0^h \int_{-\infty}^{\infty} \frac{B^+(Z)h^2 dZdY_3}{\pi[X_1{}^2+(Y_1-Y_3)^2+Z^2]^2}$$

$$+ \int_0^{\infty} \int_{-\infty}^{\infty} \frac{B_f^+(X_2)h^2 dX_2 dY_2}{\pi[(X_1-X_2)^2+(Y_1-Y_2)^2+h^2]^2} \qquad \text{3-80}$$

where Y_1, Y_2 and Y_3 represent the coordinate axes perpendicular to the plane of the paper for surfaces one, two and three, respectively. After integrating equation (3-80) yields

$$B_f^+(X_1) = q(X_1) + \frac{1}{2}\sigma T_b{}^4 \left[1 - \frac{X_1}{\sqrt{X_1{}^2+h^2}}\right] + \frac{1}{2}\int_0^{\infty} \frac{B_f^+(X_2)h^2 dX_2}{[(X_1-X_2)^2+h^2]^{3/2}} \, . \qquad \text{3-81}$$

Again introducing $x = X_1/h$, $y = X_2/h$, and assuming the specified heat flux decays exponentially, i.e., $q(X_1) = q_0\exp(-mx)$, the integral equation (3-81) takes the form of

$$B_f^*(x,m) = q_0 e^{-mx} + \frac{\sigma}{2} T_b{}^4 \left[1 - \frac{x}{\sqrt{x^2+1}}\right] + \frac{1}{2}\int_0^{\infty} B_f^*(y,m)K(|x-y|)dy \qquad \text{3-82}$$

where

$$K(|x-y|) = K(x,y) = \frac{1}{[(x-y)^2+1]^{3/2}} \, .$$

Using superposition, the solution of equation (3-82) can be written as

$$B_f^*(x,m) = q_0 B(x,m) + \sigma T_b{}^4 \phi(x) \qquad \text{3-83}$$

where $B(x,m)$ and $\phi(x)$ are evaluated for $\rho=1$ from equations (3-8) and (3-9) respectively. Replacing $\phi(y)$ by 1.0 using equation (3-64), equation (3-9) for $\rho = 1.0$ becomes

$$\phi(x) = \frac{1}{2}\left[1 - \frac{x}{\sqrt{x^2+1}}\right] + \frac{1}{2}\left[1 + \frac{x}{\sqrt{x^2+1}}\right] = 1 \qquad 3\text{-}84$$

Thus for $\rho = 1$, the dimensionless radiosity $\phi(x)$ is unity. Therefore equation (3-83) reduces to

$$B_f^*(x,m) = q_0 B(x,m) + \sigma T_b^{\ 4} \quad . \qquad 3\text{-}85$$

The heat flux specified for surface one can be expressed in terms of radiosity and emissive power as

$$q(x) = \frac{\varepsilon}{\rho}\left[\sigma T^4(x) - B_f^*(x,m)\right] \quad . \qquad 3\text{-}86$$

Solving equation (3-86) for the emissive power yields

$$\sigma T^4(x) = \frac{\rho}{\varepsilon}\, q_0 e^{-mx} + q_0 B(x,m) + \sigma T_b^{\ 4} \quad . \qquad 3\text{-}87$$

The temperature distribution $T(x)$ can be determined from equation (3-87). Thus, the solutions of section A and E are interrelated.

IV. NUMERICAL RESULTS

The major portion of the problem is solved analytically in the previous chapter. The analysis yielded radiosity and heat flux from the cavity in terms of universal functions. Numerical results for the H-Functions, dimensionless radiosity $B(x,m)$ and $\phi(x)$, local heat flux q and overall heat transfer Q^*, apparent emittance $\varepsilon_a(x)$ and overall apparent emittance $\overline{\varepsilon}_a(m)$ are computed and are presented in this chapter. The H-Functions are determined from a nonlinear Fredholm integral equation using successive approximations. The integro-differential equation for the radiosity of the cavity is solved numerically by Runge-Kutta method. IBM 360 model 50 digital computer is employed to solve these integral and differential equations. The details of the numerical techniques are explained in this chapter.

A. COMPUTATION OF H-FUNCTIONS.

The integral equation selected for the numerical computation of the H-Functions is

$$\frac{1}{H(m)} = \sqrt{1-\rho} + \frac{\rho}{2}\int_0^\infty \frac{mJ_1(n)H(n)}{n+m}\,dn \,. \qquad 4\text{-}1$$

Equation (4-1) can also be expressed as

$$H(m) = 1 + \frac{\rho}{2}\,H(m)\int_0^\infty \frac{nJ_1(n)H(n)}{n+m}\,dn \qquad 4\text{-}2$$

For convenience equations (3-52) and (3-43) are rewritten as equations (4-1) and (4-2). Experience with similar equations in gaseous radiative transfer indicates that equation (4-1) is more suitable for iterative solution. Application of the method of successive approximation to equation (4-1) yields

$$\frac{1}{H_{K+1}(m)} = \sqrt{1-\rho} + \frac{\rho}{2}\int_0^\infty \frac{mJ_1(n)H_K(n)}{n+m}\,dn \; . \qquad 4\text{-}3$$

Since the minimum value of the integral term of equation (4-2) is zero, the H-function is greater than or equal to unity. Therefore, the initial value for the H-function is assumed to be

$$H_1(m) = 1.0 \quad . \qquad 4\text{-}4$$

The integrand of the integral term in equation (4-3) depends on m and H(m). Replacing the integral term by Gaussian quadrature of order N, equation (4-3) takes the form

$$\frac{1}{H_{K+1}(m)} = \sqrt{1-\rho} + \rho F\left[m,\ H_K(n_1),\ H_K(n_2),\ H_K(n_3),\ \cdot\cdot\cdot,\ H_K(n_N)\right] \qquad 4\text{-}5$$

where F represents the numerical quadrature with quadrature points n_1, n_2, n_3, • • •, n_N. In the iterative technique used to solve equation (4-5) the most recent values of $H_{K+1}(m)$ are preferred to those of $H_K(m)$ for the use in the right side of the equation. The iterative procedure is as follows

$$\frac{1}{H_{K+1}(m_1)} = \sqrt{1-\rho} + \rho F\left[m_1,\ H_K(n_1),\ H_K(n_2),\ H_K(n_3),\ \cdot\cdot\cdot,\ H_K(n_N)\right]$$

$$\frac{1}{H_{K+1}(m_2)} = \sqrt{1-\rho} + \rho F\left[m_2,\ H_{K+1}(n_1),\ H_K(n_2),\ H_K(n_3),\ \cdot\cdot\cdot,\ H_K(n_N)\right]$$

$$\frac{1}{H_{K+1}(m_3)} = \sqrt{1-\rho} + \rho F\left[m_3,\ H_{K+1}(n_1),\ H_{K+1}(n_2),\ H_K(n_3),\ \cdot\cdot\cdot,\ H_K(n_N)\right]$$

$$\vdots \qquad \vdots \qquad \vdots$$

$$\frac{1}{H_{K+1}(n_N)} = \sqrt{1-\rho} + \rho F\left[m_N, H_{K+1}(n_1), H_{K+1}(n_2), H_{K+1}(n_3), \cdot\cdot\cdot, H_{K+1}(n_{N-1}), H_K(n_N)\right]$$

where $m_1, m_2, m_3, \cdots, m_N$ are the quadrature points.

After performing the above mentioned up-dating procedure for the first iteration, the same procedure is repeated for the next iteration. The iterative process is terminated when the required accuracy of

$$|H_{K+1}(m) - H_K(m)| \leq 0.5 \times 10^{-6}$$

is obtained at all the quadrature points. The number of iterations depends upon the value of reflectance ρ. For instance five interations are enough $\rho = 0.1$, while nineteen iterations are required for $\rho = 1.0$.

Using the final values of $H(n_1), H(n_2), \cdots, H(n_N)$ the H-function is computed for even values of m with the help of equation (4-5) as follows

$$\frac{1}{H(m)} = \sqrt{1-\rho} + \rho F\left[m, H(n_1), H(n_2), H(n_3), \cdots, H(n_N)\right] . \qquad 4\text{-}6$$

The most complex and critical part in each of the iterations in the computation of the integral term in equation (4-1). Since $J_1(n)$ is contained in the integrand, i.e.,

$$f(n) = \frac{mJ_1(n)H(n)}{n+m} ,$$

the function f(n) oscillates slowly about the abscissa as shown in Figure 4.1. Consequently the integral term in equation (4-1) in each half cycle is smaller in absolute magnitude than, and opposite in sign to, that of the preceeding half cycle. Using Longman's [24] method for computing infinite integrals of oscillatory functions with Euler's transformation, the present integration can be expressed as slowly convergent alternating series

$$\int_0^\infty f(n)dn \simeq \int_{r_0=0}^{r_1} f(n)dn - \left[V_0 - V_1 + V_2 - V_3 + - \cdot \cdot \cdot \cdot + V_M\right] \qquad 4\text{-}7$$

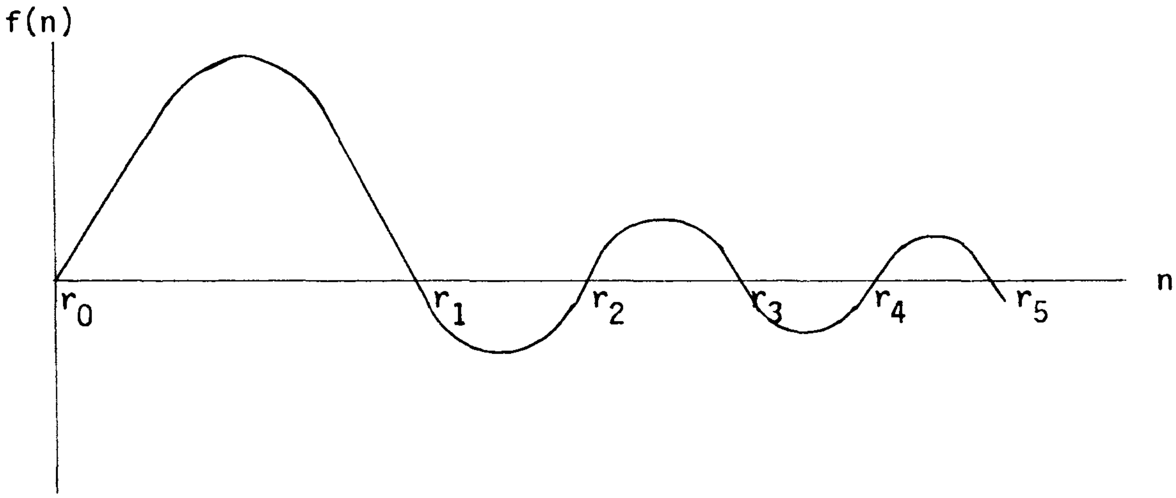

Figure 4.1 - Kernel f(n) for the integral equation

where

$$V_0 = \int_{r_1}^{r_2} |f(n)|dn \quad , \quad V_1 = \int_{r_2}^{r_3} |f(n)|dn \quad , \cdot \cdot \cdot , \; V_M = \int_{r_{M+1}}^{r_{M+2}} |f(n)|dn$$

and r_0, r_1, r_2, $\cdot \cdot \cdot$ are the roots of $J_1(n)$ and hence of $f(n)$.

Since the series, $V_0 - V_1 + V_2 - V_3 + - \cdot \cdot \cdot \cdot + V_M$, is slowly convergent alternating, then

$$V_K > 0 \quad , \quad V_{K+1} < V_K \quad , \quad \text{for all } K \quad ,$$

and if

$$\Delta V_K = V_{K+1} - V_K \qquad ; \qquad \Delta^{\rho+1} V_K = \Delta^{\rho} V_{K+1} - \Delta^{\rho} V_K \quad ,$$

then according to Euler's transformation,

$$\sum_{K=0}^{\infty} (-1)^K V_K = \frac{1}{2} V_0 - \frac{1}{4} \Delta V_0 + \frac{1}{8} \Delta^2 V_0 - + \cdot \cdot \cdot \qquad \text{4-8}$$

where the series on the right side of equation (4-8) can be shown convergent whenever the original series is convergent. Equation (4-7) can be written as

$$\int_{0}^{\infty} f(n)dn \simeq \int_{r_0=0}^{r_1} f(n)dn - \left[\frac{1}{2} V_0 - \frac{1}{4} \Delta V_0 + \frac{1}{8} \Delta^2 V_0 - + \cdot \cdot \cdot \right]. \qquad 4\text{-}9$$

A sub-program was written to perform the integration according to equation (4-9). The results for $M = 10$ are accurate to sixth decimal place.

Gaussian quadrature is used to perform the integration of each term of right side of equation (4-9). Since the H-function decays rapidly in the interval $0 \leq n \leq r_1$, the first integral term on the right side of the equation (4-7) may be broken into two terms as

$$\int_{r_0=0}^{r_1} f(n)dn = \int_{r_0=0}^{(r_1-r_0)/2} f(n)dn = \int_{(r_1-r_0)/2}^{r_1} f(n)dn \qquad 4\text{-}10$$

or

$$\int_{r_0=0}^{r_1} f(n)dn = \sum_{i=1}^{N_0} A_i f(n_i) + \sum_{i=1}^{N_1} A_i f(n_i) \qquad 4\text{-}11$$

where $N_0 = 11$ and $N_1 = 5$. Eleven point quadrature is used for evaluating the first integral term on the right side of equation (4-10) to obtain better accuracy. V_0, V_1, V_2, • • • in equation (4-7) are computed using five point Gausian quadrature.

The values of the H-function at the quadrature points and at even values of m are presented in Tables 4.1 and 4.2. The H-functions are used as initial conditions to solve the integro-differential equation for radiosity. Moments of the H-function α_0 and α_1 are computed using Longman's method and are presented in Table 4.3. The zeroth moment

Table 4.1

H-function

m	ρ = 0.10	ρ = 0.50	ρ = 0.90	ρ = 0.99	ρ = 1.00
0.000	1.05409	1.41421	3.47850	10.0000	∞
0.001	1.05404	1.41361	3.15466	9.88537	541.951
0.005	1.05381	1.41126	3.12518	9.46536	119.173
0.010	1.05354	1.40838	3.09009	9.00664	63.7505
0.020	1.05300	1.40285	3.02467	8.24719	34.6171
0.030	1.05249	1.39755	2.96452	7.63780	24.4080
0.040	1.05199	1.39246	2.90879	7.13463	19.12878
0.050	1.05150	1.38755	2.85687	6.71041	15.87818
0.060	1.05103	1.38280	2.80829	6.34692	13.66457
0.070	1.05057	1.37821	2.76266	6.03132	12.05448
0.080	1.05012	1.37376	2.71968	5.75429	10.82757
0.090	1.04968	1.36944	2.67910	5.50886	9.85968
0.100	1.04925	1.36525	2.64067	5.28967	9.07537
0.200	1.04542	1.32881	2.34274	3.92428	5.38887
0.300	1.04221	1.29972	2.14253	3.24255	4.06720
0.400	1.03946	1.27569	1.99682	2.82739	3.37438
0.500	1.03706	1.25538	1.88527	2.54575	2.94374
0.600	1.03494	1.23792	1.79675	2.34115	2.64849
0.700	1.03305	1.22272	1.72461	2.18529	2.43267
0.800	1.03136	1.20936	1.66457	2.06234	2.26762
0.900	1.02983	1.19749	1.61377	1.96273	2.13708
1.000	1.02843	1.18688	1.57018	1.88030	2.03113
2.000	1.01926	1.12090	1.33214	1.47331	1.53341
3.000	1.01444	1.08864	1.23278	1.32194	1.35811
4.000	1.01149	1.06962	1.17841	1.24300	1.26857
5.000	1.00951	1.05715	1.14424	1.19469	1.21437
6.000	1.00809	1.04837	1.12086	1.16216	1.17813
7.000	1.00703	1.04188	1.10389	1.13882	1.15224
8.000	1.00621	1.03690	1.09104	1.12127	1.13284
9.000	1.00556	1.03295	1.08097	1.10762	1.11777
10.000	1.00503	1.02976	1.07289	1.09670	1.10575
15.000	1.00340	1.01999	1.04852	1.06404	1.06989
20.000	1.00256	1.01503	1.03631	1.04781	1.05213
25.000	1.00205	1.01203	1.02900	1.03813	1.04155
30.000	1.00171	1.01003	1.02413	1.03170	1.03454
35.000	1.00147	1.00860	1.02066	1.02713	1.02955
40.000	1.00129	1.00752	1.01806	1.02370	1.02581
45.000	1.00114	1.00669	1.01604	1.02105	1.02292
50.000	1.00103	1.00602	1.01443	1.01893	1.02061
100.000	1.00051	1.00301	1.00719	1.00942	1.01025
200.000	1.00026	1.00150	1.00359	1.00470	1.00511
300.000	1.00017	1.00100	1.00239	1.00313	1.00341
400.000	1.00013	1.00075	1.00179	1.00235	1.00255
500.000	1.00010	1.00060	1.00143	1.00188	1.00204
1000.000	1.00005	1.00030	1.00072	1.00094	1.00102

Table 4.2

H-function at quadrature points

m	ρ = 0.10	ρ = 0.50	ρ = 0.90	ρ = 0.99	ρ = 1.00
0.00544	1.05379	1.41100	3.12200	9.42206	110.295
0.02823	1.05257	1.39847	2.97480	7.73670	25.7072
0.06746	1.05068	1.37936	2.77398	6.10744	12.4203
0.12023	1.04841	1.35711	2.56880	4.91040	7.86778
0.18261	1.04603	1.33453	2.38569	4.09130	5.75490
0.25000	1.04375	1.31352	2.23394	3.53569	4.60444
0.31739	1.04170	1.29523	2.11403	3.15663	3.91764
0.37977	1.03999	1.28021	2.02306	2.89792	3.48696
0.43254	1.03864	1.26872	1.95744	2.72470	3.21393
0.47177	1.03771	1.26079	1.91406	2.61575	3.04806
0.49456	1.03718	1.25640	1.89067	2.55875	2.96299
0.65629	1.03385	1.22912	1.75444	2.24862	2.51946
1.26884	1.02524	1.16320	1.47862	1.71560	1.82480
2.16585	1.01826	1.11409	1.31037	1.43930	1.49360
3.06287	1.01421	1.08716	1.22844	1.31554	1.35080
3.67542	1.01231	1.07487	1.19313	1.26418	1.29240
3.98107	1.01153	1.06991	1.17921	1.24414	1.26985
4.56644	1.01028	1.06198	1.15735	1.21311	1.23500
5.42365	1.00885	1.05308	1.13334	1.17947	1.19739
6.28086	1.00776	1.04636	1.11557	1.15486	1.17002
6.86623	1.00716	1.04265	1.10588	1.14155	1.15526
7.16373	1.00688	1.04098	1.10155	1.13561	1.14869
7.74432	1.00641	1.03806	1.09402	1.12533	1.13732
8.59453	1.00581	1.03445	1.08478	1.11277	1.12345
9.44474	1.00531	1.03145	1.07717	1.10248	1.11211
10.0253	1.00502	1.02968	1.07271	1.09645	1.10548
10.3212	1.00488	1.02886	1.07062	1.09364	1.10239
10.9004	1.00463	1.02736	1.06686	1.08859	1.09683
11.7486	1.00431	1.02543	1.06202	1.08209	1.08969
12.5967	1.00403	1.02375	1.05783	1.07648	1.08357
13.1759	1.00386	1.02272	1.05528	1.07306	1.07978
13.4713	1.00378	1.02223	1.05406	1.07143	1.07799
14.0499	1.00362	1.02133	1.05182	1.06844	1.07471
14.8972	1.00343	1.02013	1.04885	1.06449	1.07038
15.7444	1.00324	1.01906	1.04621	1.06096	1.06652
16.3230	1.00313	1.01839	1.04456	1.05877	1.06412
16.6182	1.00307	1.01806	1.04376	1.05770	1.06295
17.1964	1.00297	1.01746	1.04228	1.05573	1.06080
18.0432	1.00284	1.01665	1.04028	1.05308	1.05789
18.8900	1.00271	1.01591	1.03846	1.05066	1.05525

Table 4.2 (continued)

H-function at quadrature points

m	ρ = 0.10	ρ = 0.50	ρ = 0.90	ρ = 0.99	ρ = 1.00
19.4683	1.00263	1.01544	1.03731	1.04914	1.05358
19.7634	1.00259	1.01521	1.03675	1.04839	1.05277
20.3414	1.00252	1.01478	1.03570	1.04700	1.05124
21.1880	1.00242	1.01419	1.03426	1.04509	1.04916
22.0345	1.00233	1.01365	1.03293	1.04333	1.04724
22.6126	1.00227	1.01330	1.03208	1.04221	1.04601
22.9075	1.00224	1.01313	1.03167	1.04166	1.04541
23.4855	1.00218	1.01281	1.03088	1.04062	1.04428
24.3319	1.00211	1.01236	1.02980	1.03919	1.04271
25.1782	1.00204	1.01195	1.02879	1.03785	1.04125
25.7562	1.00199	1.01168	1.02814	1.03699	1.04031
26.0511	1.00197	1.01155	1.02782	1.03657	1.03985
26.6290	1.00193	1.01130	1.02721	1.03577	1.03897
27.4752	1.00187	1.01095	1.02637	1.03465	1.03776
28.3215	1.00181	1.01062	1.02557	1.03360	1.03661
28.8994	1.00178	1.01041	1.02506	1.03292	1.03587
29.1943	1.00176	1.01031	1.02480	1.03259	1.03550
29.7721	1.00173	1.01011	1.02432	1.03195	1.03480
30.6182	1.00168	1.00983	1.02364	1.03105	1.03383
31.4644	1.00163	1.00956	1.02300	1.03021	1.03291
32.0422	1.00160	1.00939	1.02258	1.02966	1.03231
32.3371	1.00159	1.00930	1.02237	1.02938	1.03201
32.9149	1.00156	1.00914	1.02198	1.02886	1.03144
33.7610	1.00152	1.00891	1.02142	1.02813	1.03064
34.6071	1.00149	1.00869	1.02090	1.02744	1.02988
35.1849	1.00146	1.00855	1.02055	1.02698	1.02939

calculated in this manner agrees with the exact value which is given by equation (3-51).

Table 4.3

Moments of the H-function

ρ	α_0	α_1
0	1.00000	1.00000
0.10	1.02633	1.03025
0.50	1.17157	1.20488
0.90	1.51949	1.70456
0.99	1.81818	2.36345
1.00	2.00000	3.83338

B. RADIOSITY VARIATION INTO CAVITY.

B(x,m) can be determined from the integro-differential equation (3-26)

$$\frac{\partial B(x,m)}{\partial x} = - mB(x,m) + \frac{\rho}{2} H(m) \int_0^\infty nB(x,n)J_1(n)dn$$

with the initial condition, $B(o,m) = H(m)$. The integro-differential equation (3-26) takes the form

$$\frac{\partial B(x,m)}{\partial x} = - mB(x,m) + \frac{\rho}{2} H(m)\Phi(x) \qquad 4\text{-}14$$

where from equation (3-60)

$$\Phi(x) = \int_0^\infty nB(x,n)J_1(n)dn \quad .$$

The partial differential equation (4-14) can be expressed as a system of ordinary differential equations:

$$\frac{dB_1(x)}{dx} = - m_1 B_1(x) + \frac{\rho}{2} H_1 \Phi(x)$$

$$\frac{dB_2(x)}{dx} = - m_2 B_2(x) + \frac{\rho}{2} H_2 \Phi(x)$$

$$\begin{array}{ccc} \cdot & \cdot & \cdot \\ \cdot & \cdot & \cdot \\ \cdot & \cdot & \cdot \end{array} \qquad 4\text{-}15$$

$$\frac{dB_N(x)}{dx} = - m_N B_N(x) + \frac{\rho}{2} H_N \Phi(x)$$

where

$$\Phi(x) = S\left[B_1, B_2, \cdot \cdot \cdot, B_N\right] \qquad 4\text{-}16$$

and

$$B_i(x) = B(x, m_i)$$

$$H_i = H(m_i) \quad . \qquad 4\text{-}17$$

The quantity S represents Longman's numerical quadrature with quadrature points m_1, m_2, $\cdot \cdot \cdot$, m_N. Thus $B(x,m)$ and $\Phi(x)$ are coupled in such a manner that $B(x,m)$ must be computed at all quadrature points to determine the value of $\Phi(x)$. In order to obtain $B(x,m)$ at even values of m, additional differential equations must be solved. Evaluating equation (4-14) at $m_{N+1} = 0$, $m_{N+2} = .001$, $m_{N+3} = 0.005$, $\cdot \cdot \cdot$, $m_{NN} = 1000.0$ yields

$$\frac{dB_{N+1}(x)}{dx} = - m_{N+1} B_{N+1}(x) + \frac{\rho}{2} H_{N+1} \Phi(x)$$

$$\frac{dB_{N+2}(x)}{dx} = - m_{N+2} B_{N+2}(x) + \frac{\rho}{2} H_{N+2} \Phi(x)$$

$$\begin{array}{ccc} \cdot & \cdot & \cdot \\ \cdot & \cdot & \cdot \\ \cdot & \cdot & \cdot \end{array} \qquad 4\text{-}18$$

$$\frac{dB_{NN}(x)}{dx} = - m_{NN} B_{NN}(x) + \frac{\rho}{2} H_{NN} \Phi(x) \quad .$$

The dimensionless radiosity $\phi(x)$ is calculated from an additional differential equation (3-60)

$$\frac{d\phi(x)}{dx} = -\frac{1}{2}\phi(x) + \frac{\rho}{4}\alpha_0\varphi(x) \ .$$

Thus, a system of NN+1 ordinary differential equations must be solved.

Runga-Kutta Simpson's method (one third rule) [25] has been used to solve the differential equations for the dimensionless radiosity $B(x,m)$ and $\phi(x)$. In this method the error is of the order h^4, where h is step size. By using h = 0.05, quite accurate results are obtained and the method seems to be economical as far as computer time is concerned.

The dimensionless radiosity $B(x,m)$ for m = 0 and m = 1 at various depths within the cavity is presented in Tables 4.4 and 4.5. Values of $\phi(x)$ and $\varphi(x)$ at various depths in the cavity are listed in Tables 4.6 and 4.7.

The variation of radiosity $B(x,m)$ with the temperature distribution parameter m is presented in Figures 4.2 through 4.8 for fixed depths into the cavity of x = 0, 0.1, 0.5, 1.0, 2.0, 3.0 and 4.0. Each figure has five curves corresponding to ρ = 0.1, 0.5, 0.9, 0.99 and 1.0. The general trends of these seven plots are

1. The maximum value of the radiosity occurs when the cavity is isothermal, m = 0.
2. The radiosity increases as the reflectance ρ is increased. Small changes in ρ from unity cause large changes in B when m is small.

Table 4.4

Dimensionless radiosity $B(x,m)$ for isothermal cavity

x	ρ = 0.1	ρ = 0.5	ρ = 0.9	ρ = 0.99
0.0	1.05409	1.41421	3.16228	10.0000
0.01	1.05463	1.41846	3.18499	10.0940
0.05	1.05681	1.43550	3.27657	10.4742
0.10	1.05951	1.45681	3.39231	10.9575
0.20	1.06478	1.49895	3.62587	11.9432
0.30	1.06978	1.53967	3.85864	12.9420
0.40	1.07441	1.57820	4.08706	13.9409
0.50	1.07861	1.61406	4.30853	14.9301
0.60	1.08235	1.64700	4.52139	15.9032
0.70	1.08566	1.67700	4.72481	16.8561
0.80	1.08856	1.70416	4.91855	17.7871
0.90	1.09108	1.72865	5.10275	18.6957
1.00	1.09327	1.75071	5.27780	19.5823
1.50	1.10060	1.83241	6.03348	23.7184
2.00	1.10440	1.88253	6.63256	27.4493
2.50	1.10653	1.91471	7.11756	30.8651
3.00	1.10781	1.93623	7.51627	34.0234
4.00	1.10919	1.96166	8.12604	39.7147
5.00	1.10987		8.56122	44.7318
6.00	1.11024		8.87916	49.2031
7.00	1.11047		9.11566	53.2173
8.00	1.11062		9.29416	56.8403
10.00	1.11080		9.53599	63.1081
12.00			9.68311	68.3145
15.00			9.80934	74.5918
20.00			9.90543	80.8500

Table 4.5

Dimensionless radiosity B(x,m) for m = 1.0

x	ρ = 0.10	ρ = 0.50	ρ = 0.90	ρ = 0.99	ρ = 1.00
0.0	1.02843	1.18688	1.57018	1.88030	2.03113
0.01	1.01873	1.17862	1.56578	1.87918	2.03160
0.05	0.98086	1.14642	1.54896	1.87558	2.03440
0.10	0.93559	1.10795	1.52947	1.87275	2.03970
0.20	0.85145	1.03617	1.49429	1.87094	2.05445
0.30	0.77507	0.97007	1.46207	1.87167	2.07187
0.40	0.70560	0.90851	1.43084	1.87224	2.08920
0.50	0.64235	0.85067	1.39929	1.87106	2.10452
0.60	0.58470	0.79602	1.36668	1.86709	2.11673
0.70	0.53212	0.74420	1.33271	1.85989	2.12533
0.80	0.48417	0.69505	1.29738	1.84946	2.13026
0.90	0.44043	0.64845	1.26092	1.83601	2.13174
1.00	0.40055	0.60434	1.22361	1.81989	2.13014
1.50	0.24842	0.41938	1.03445	1.71299	2.08999
2.00	0.15351	0.28683	0.85938	1.58888	2.02463
2.50	0.09471	0.19486	0.70916	1.46740	1.95564
3.00	0.05841	0.13217	0.58470	1.35591	1.89161
4.00	0.02229	0.06138	0.40103	1.16792	1.78662
5.00	0.00859		0.28052	1.02014	1.70955
6.00	0.00338		0.20052	0.90191	1.65250
7.00	0.00138		0.14626	0.80482	1.60892
8.00	0.00060		0.10858	0.72316	1.57438
10.00	0.00015		0.06251	0.59232	1.52235
12.00			0.03773	0.49151	1.48413
15.00			0.01901	0.37752	1.44151
20.00			0.00711	0.27101	1.39202

Table 4.6

Dimensionless radiosity $\phi(x)$

x	ρ = 0.10	ρ = 0.50	ρ = 0.90	ρ = 0.99
0.0	0.51317	0.58579	0.75975	0.90909
0.01	0.50828	0.58154	0.75722	0.90814
0.05	0.48873	0.56450	0.74705	0.90430
0.10	0.46444	0.54319	0.73419	0.89942
0.20	0.41696	0.50105	0.70824	0.88946
0.30	0.37196	0.46033	0.68237	0.87937
0.40	0.33031	0.42180	0.65699	0.86928
0.50	0.29253	0.38594	0.63238	0.85929
0.60	0.25880	0.35299	0.60873	0.84946
0.70	0.22903	0.32299	0.58613	0.83984
0.80	0.20298	0.29584	0.56460	0.83043
0.90	0.18029	0.27135	0.54414	0.82125
1.00	0.16059	0.24929	0.52469	0.81230
1.50	0.09460	0.16758	0.44072	0.77052
2.00	0.06041	0.11747	0.37416	0.73283
2.50	0.04124	0.08528	0.32027	0.69833
3.00	0.02968	0.06377	0.27597	0.66643
4.00	0.01726	0.03834	0.20822	0.60894
5.00	0.01118		0.15986	0.55826
6.00	0.00779		0.12454	0.51310
7.00	0.00572		0.09826	0.47255
8.00	0.00437		0.07842	0.43596
10.00	0.00279		0.05156	0.37264
12.00			0.03521	0.32005
15.00			0.02118	0.25675
20.00			0.01051	0.18056

Table 4.7

Function $\Phi(x)$

x	ρ = 0.10	ρ = 0.50	ρ = 0.90	ρ = 0.99	ρ = 1.00
0.0	1.03101	1.20106	1.59337	1.89527	2.04103
0.01	1.03112	1.20270	1.59821	1.90401	2.05129
0.05	1.02855	1.20614	1.61788	1.93576	2.08922
0.10	1.01868	1.20341	1.63423	1.96819	2.12950
0.20	0.97843	1.17594	1.64321	2.00929	2.18655
0.30	0.91585	1.12366	1.62411	2.02165	2.21502
0.40	0.83847	1.05373	1.58320	2.01097	2.22039
0.50	0.75394	0.97368	1.52746	1.98384	2.20909
0.60	0.66868	0.88999	1.46324	1.94635	2.18708
0.70	0.58725	0.80751	1.39549	1.90332	2.15915
0.80	0.51243	0.72935	1.32762	1.85818	2.12867
0.90	0.44548	0.65719	1.26174	1.81310	2.09783
1.00	0.38668	0.59171	1.19902	1.76934	2.06789
1.50	0.19426	0.35563	0.93981	1.58181	1.94381
2.00	0.10506	0.22372	0.75393	1.43903	1.85698
2.50	0.06143	0.14696	0.61571	1.32497	1.79315
3.00	0.03838	0.10008	0.50943	1.22983	1.74370
4.00	0.01749	0.05063	0.35867	1.07638	1.67082
5.00	0.00927		0.25946	0.95492	1.61858
6.00	0.00545		0.19149	0.85459	1.57852
7.00	0.00346		0.14359	0.76950	1.54636
8.00	0.00232		0.10912	0.69604	1.51969
10.00	0.00118		0.06517	0.57525	1.47742
12.00			0.04047	0.48012	1.44492
15.00			0.02111	0.37095	1.40746
20.00			0.00826	0.24740	1.36267

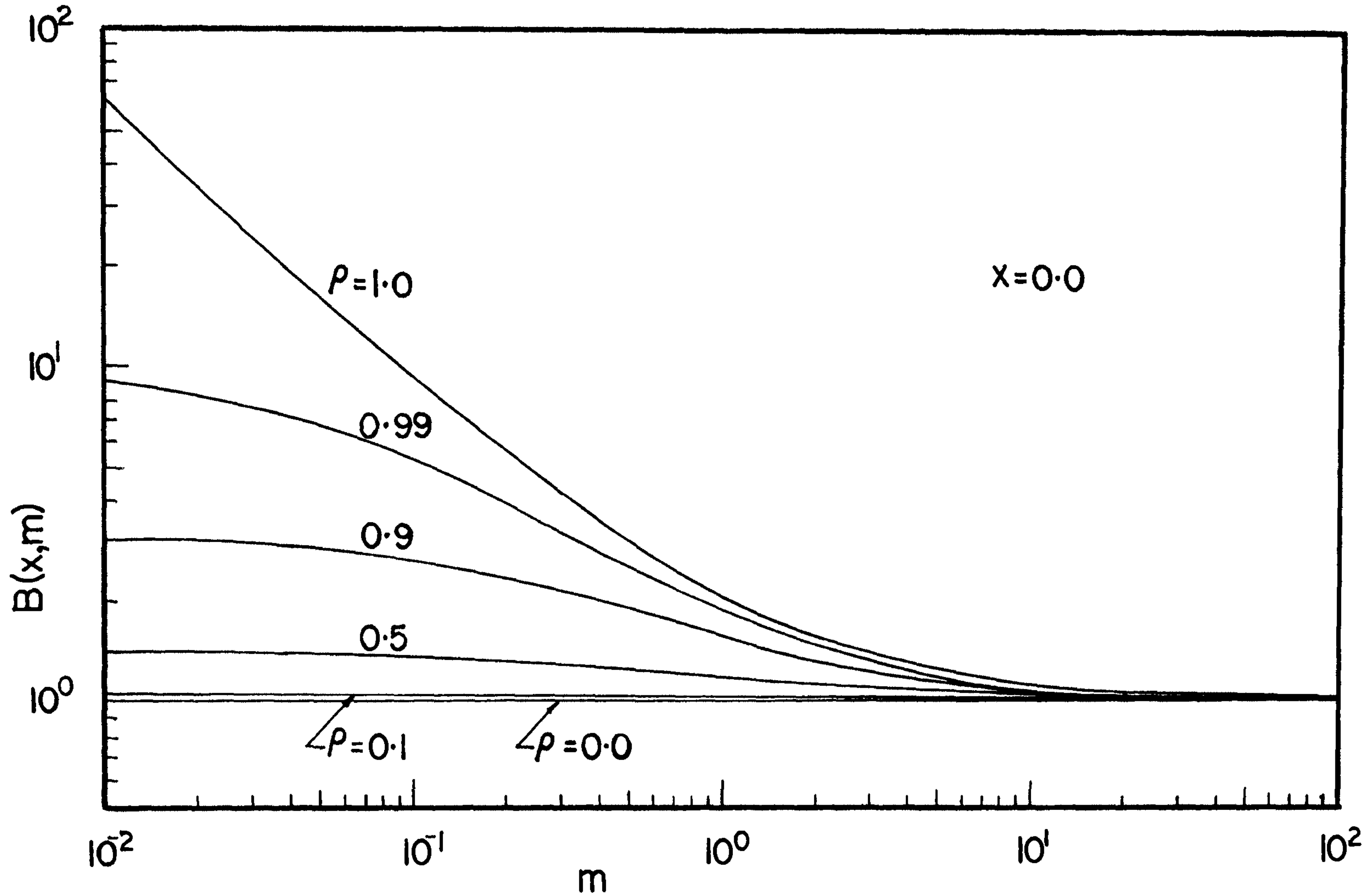

Figure 4.2 - Dimensionless radiosity B(x,m) versus m at the edge of the cavity

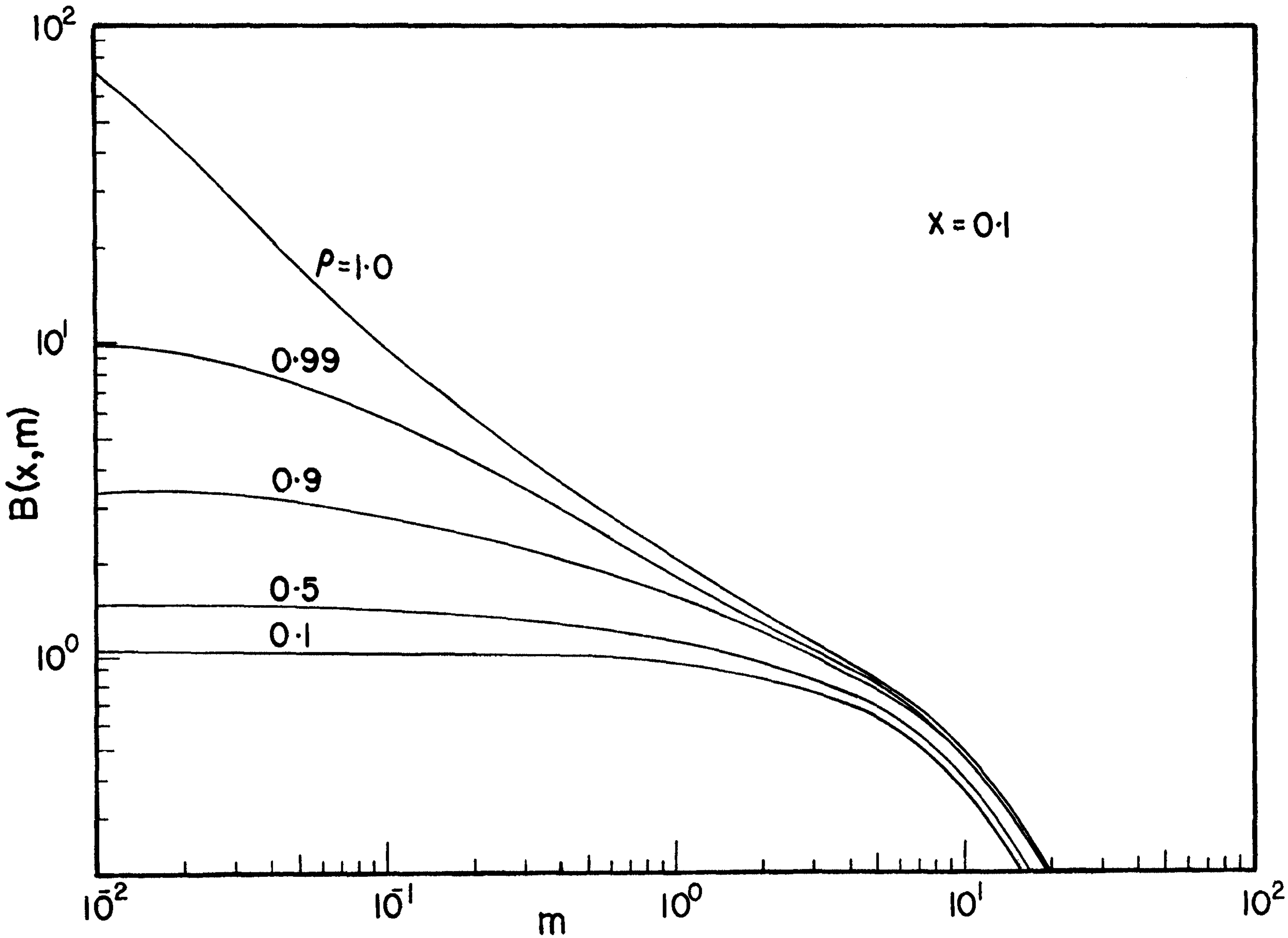

Figure 4.3 - Dimensionless radiosity B(x,m) versus m at x = 0.1

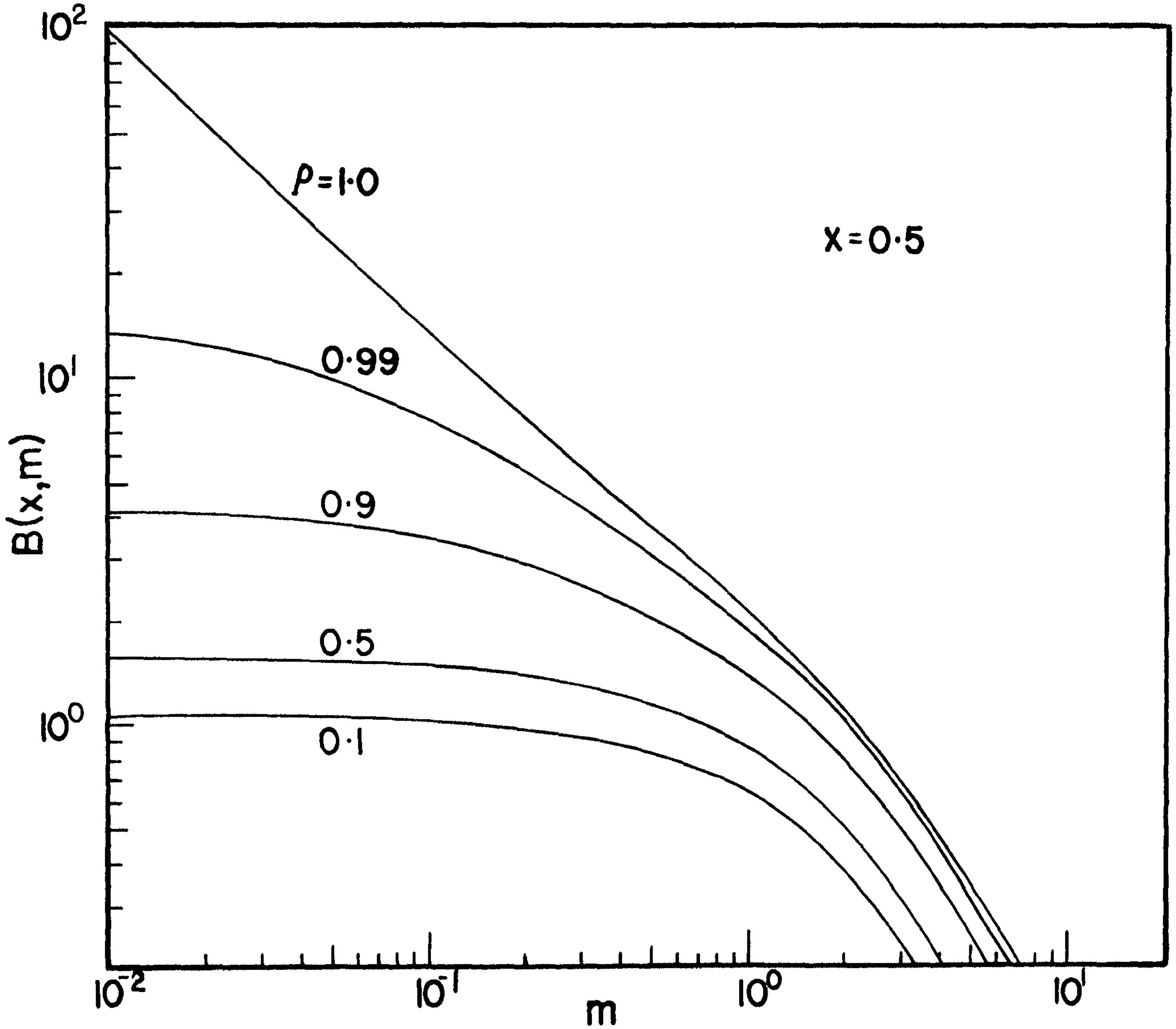

Figure 4.4 - Dimensionless radiosity $B(x,m)$ versus m at $x = 0.5$

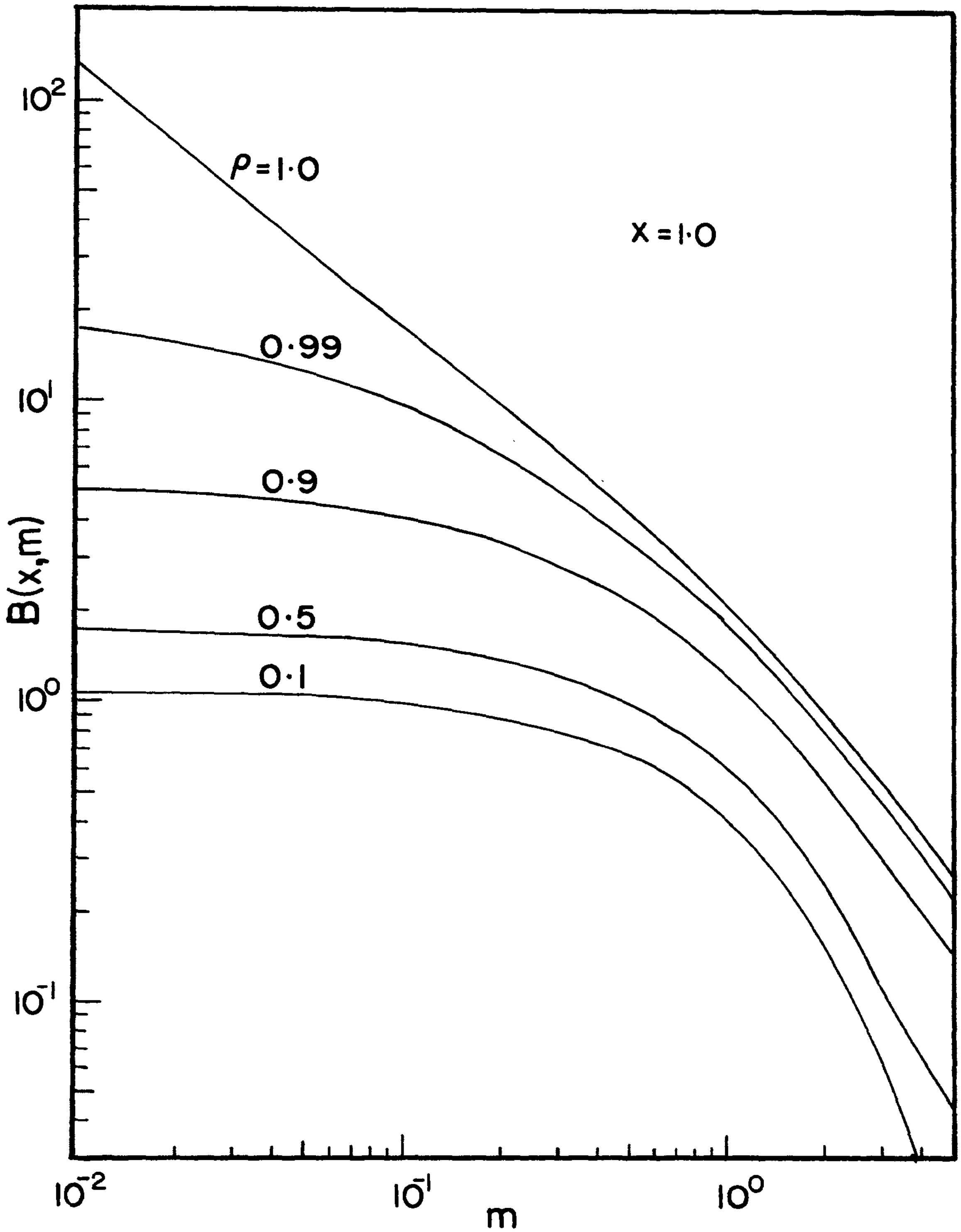

Figure 4.5 - Dimensionless radiosity B(x,m) versus m at x = 1.0

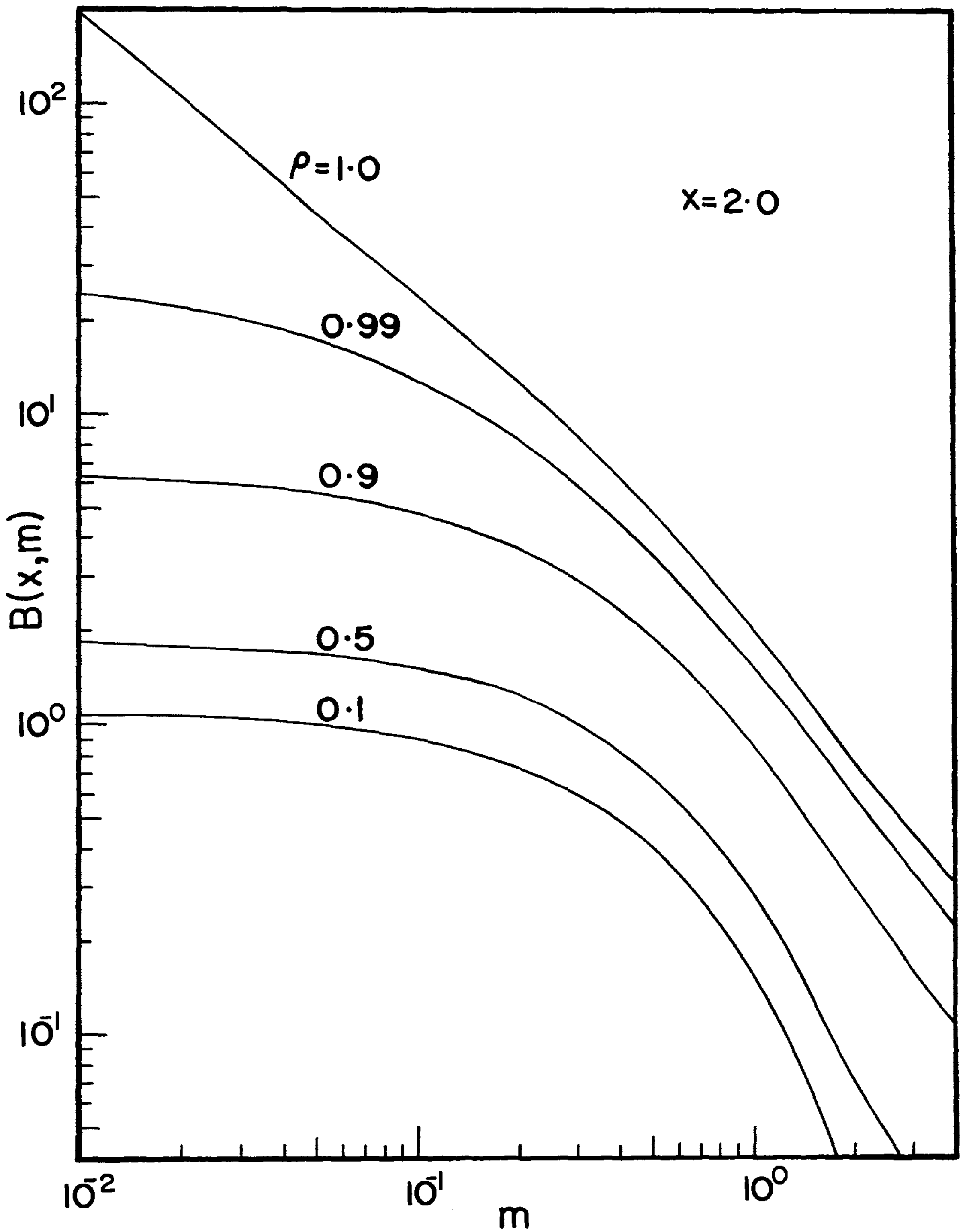

Figure 4.6 - Dimensionless radiosity B(x,m) versus m at x = 2.0

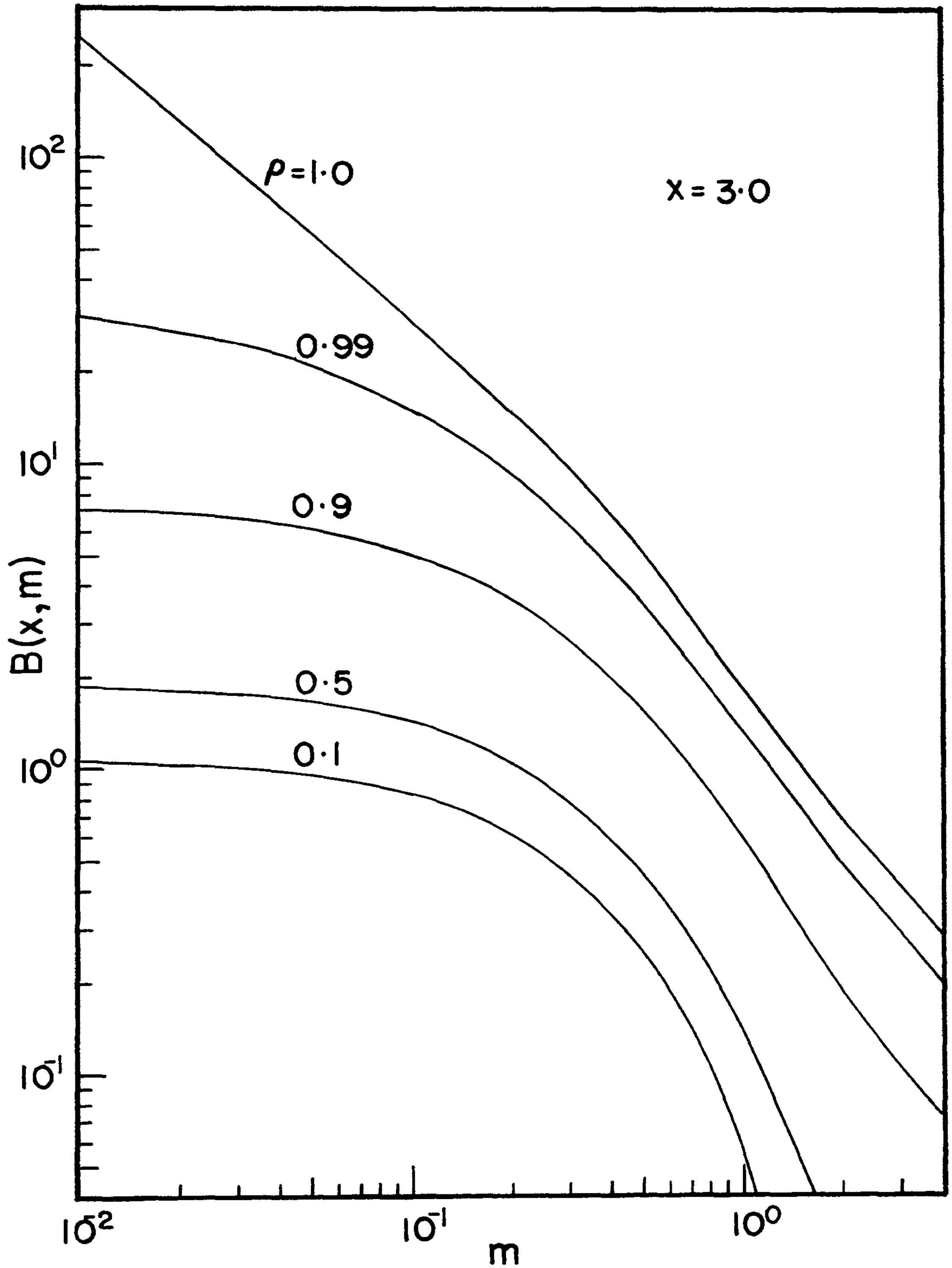

Figure 4.7 - Dimensionless radiosity B(x,m) versus m at x = 3.0

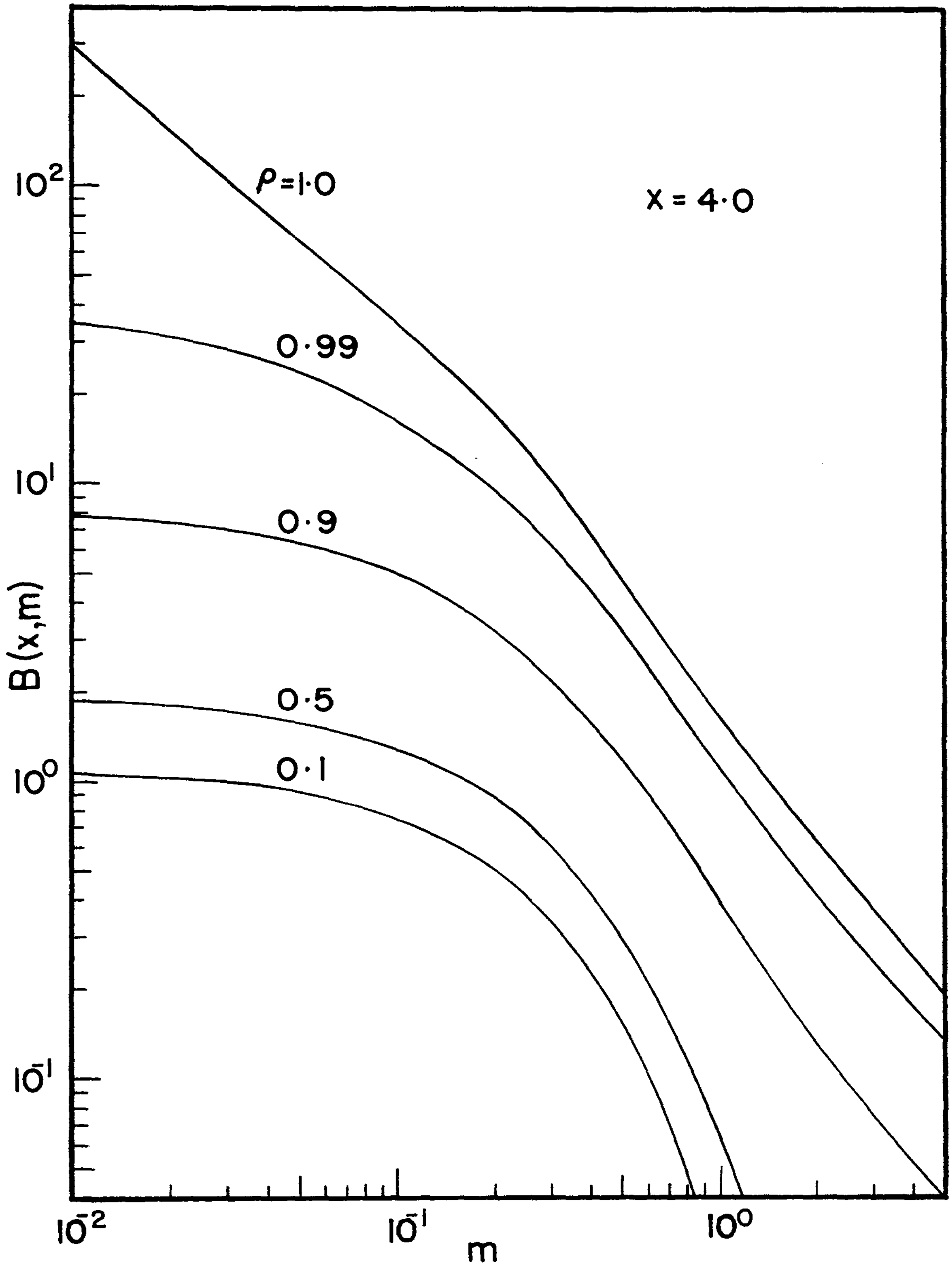

Figure 4.8 - Dimensionless radiosity B(x,m) versus m at x = 4.0

3. The higher the value of m, the lower is the value of the radiosity. As m approaches infinity, the radiosity reduces to zero except at the edge of the cavity where radiosity converges to 1.0.

The variations of the radiosity, $B(x,m)$, within the cavity are presented in Figures 4.9 through 4.13 for ρ = 0.1, 0.5, 0.9, 0.99 and 1.0, respectively. In each figure, the influence of the temperature distribution on the radiosity is illustrated by presenting results for various values of m. For given reflectance ρ the radiosity exhibits three different functional variations depending on the temperature parameter m.

1. For the isothermal case $m = 0$, the radiosity increases with depth into the cavity. Starting at the edge of the cavity with a value of $1/\sqrt{\varepsilon}$, the radiosity increases to a value of $1/\varepsilon$.
2. For small values of m, the radiosity starts rising first at $x = 0$, then upon reaching a maximum, starts to decrease with depth into the cavity.
3. For large values of m, the radiosity starts decaying right from the edge of the cavity and continues to decrease with depth. The decay of the radiosity is the steepest near the edge of the cavity.

The variation in the dimensionless radiosity $\phi(x)$ with the depth in the cavity has been plotted in Figure 4.14 for ρ = 0.1, 0.5, 0.9, 0.99 and 1.0. At $\rho = 1.0$, the radiosity $\phi(x)$ is constant at a value of unity. Figure 4.14 also shows that the larger the value of ρ, the

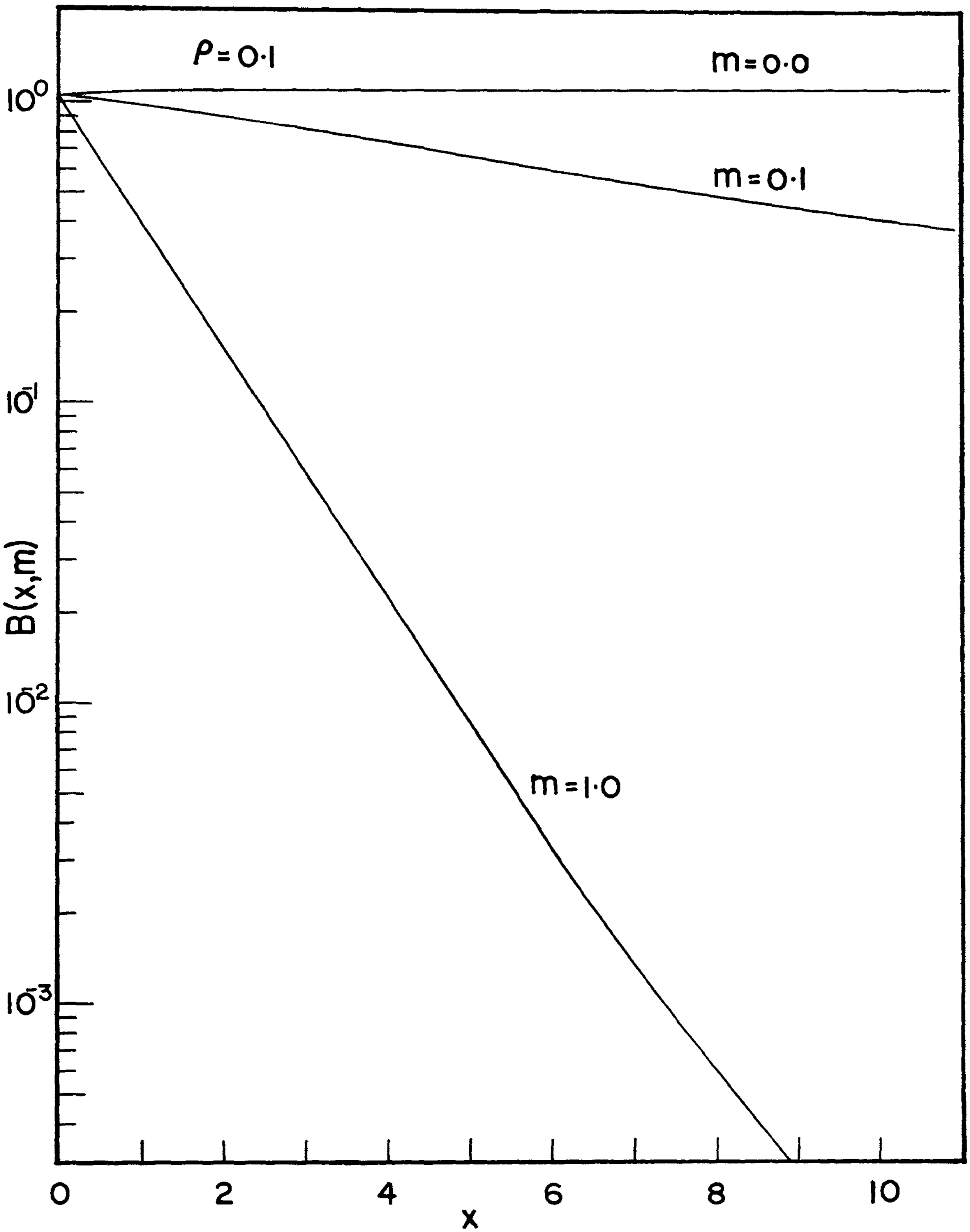

Figure 4.9 - Dimensionless radiosity B(x,m) variation within the cavity for $\rho = 0.1$

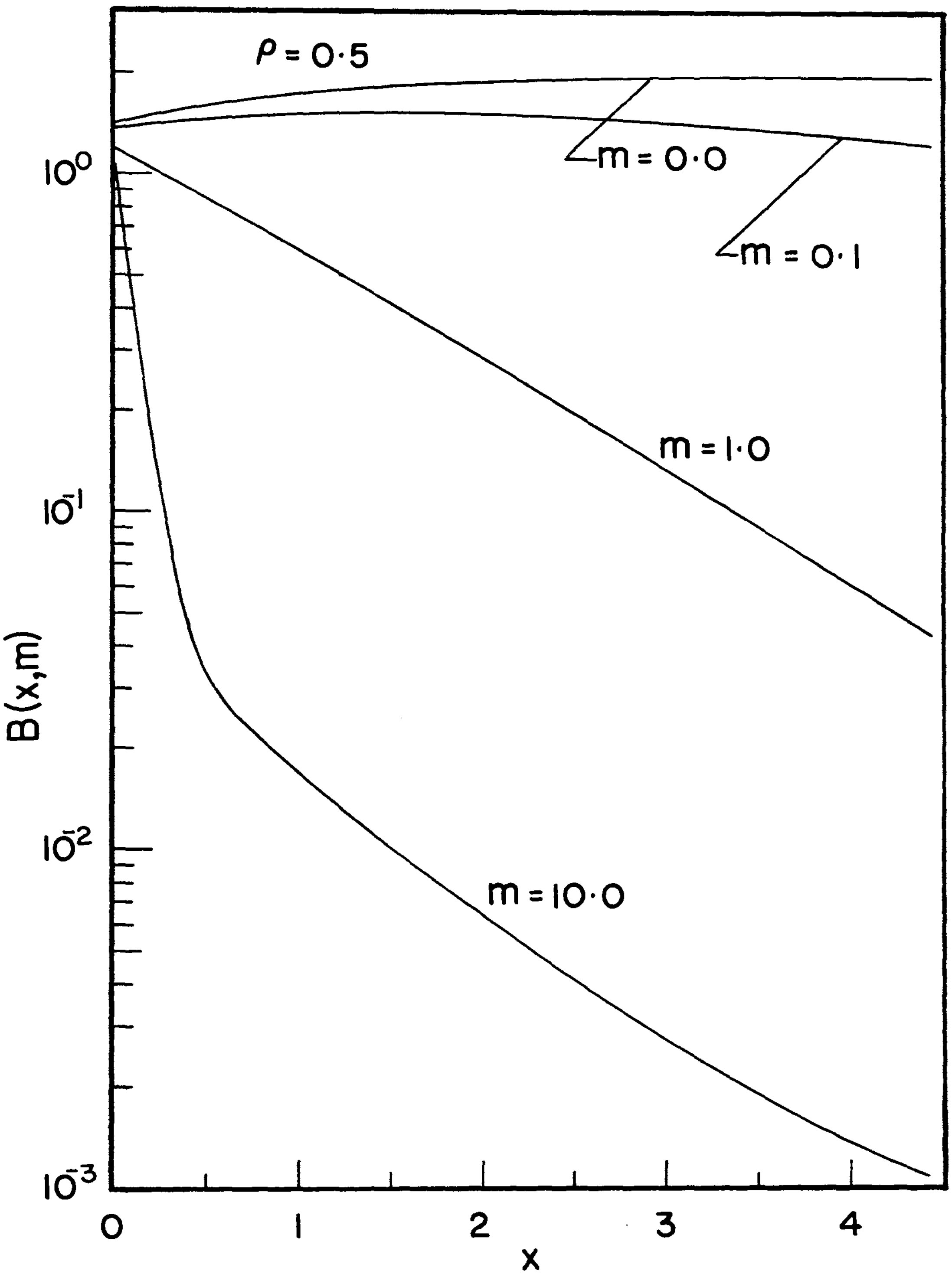

Figure 4.10 - Dimensionless radiosity B(x,m) variation within the cavity for ρ = 0.5

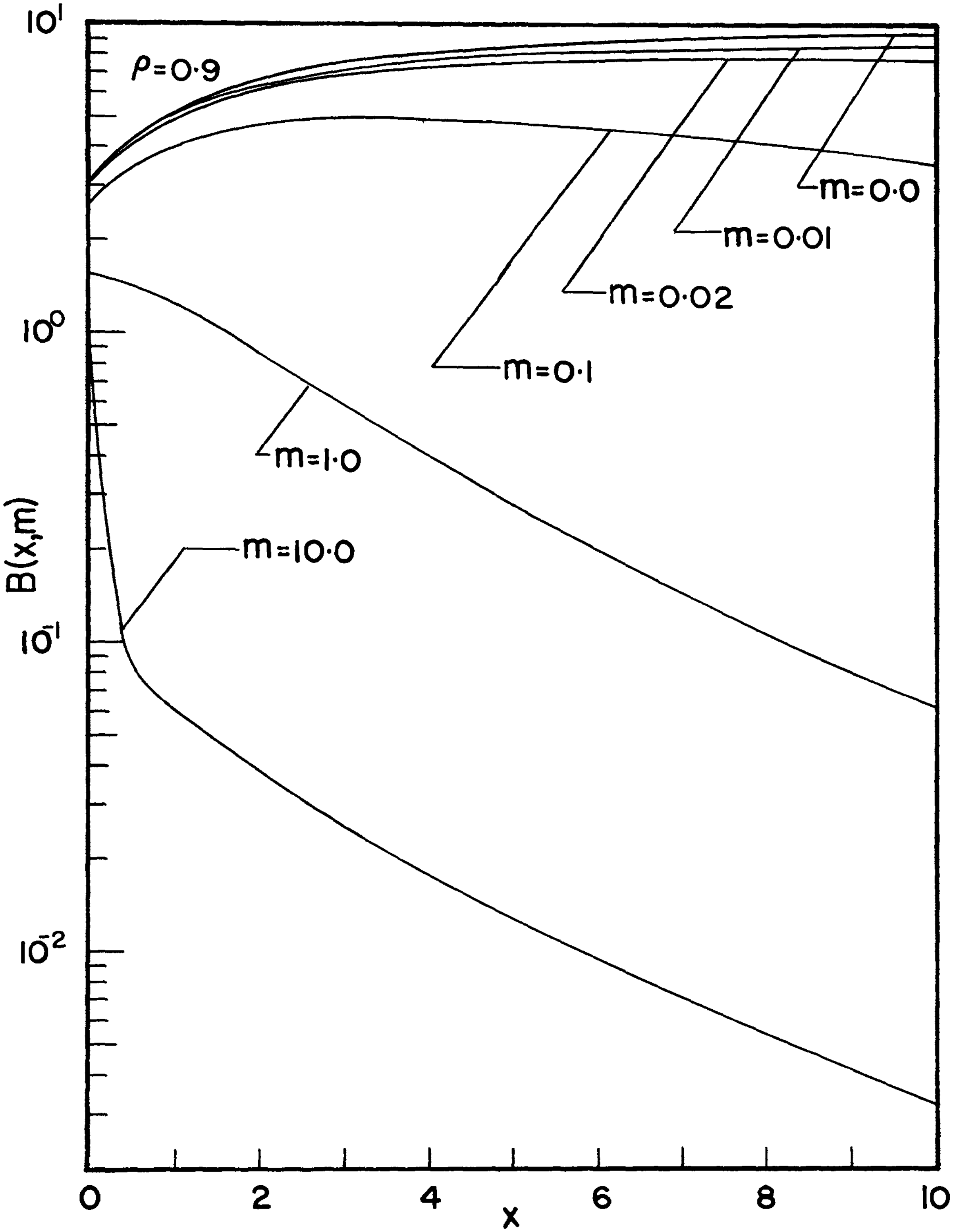

Figure 4.11 - Dimensionless radiosity B(x,m) variation within the cavity for $\rho = 0.9$

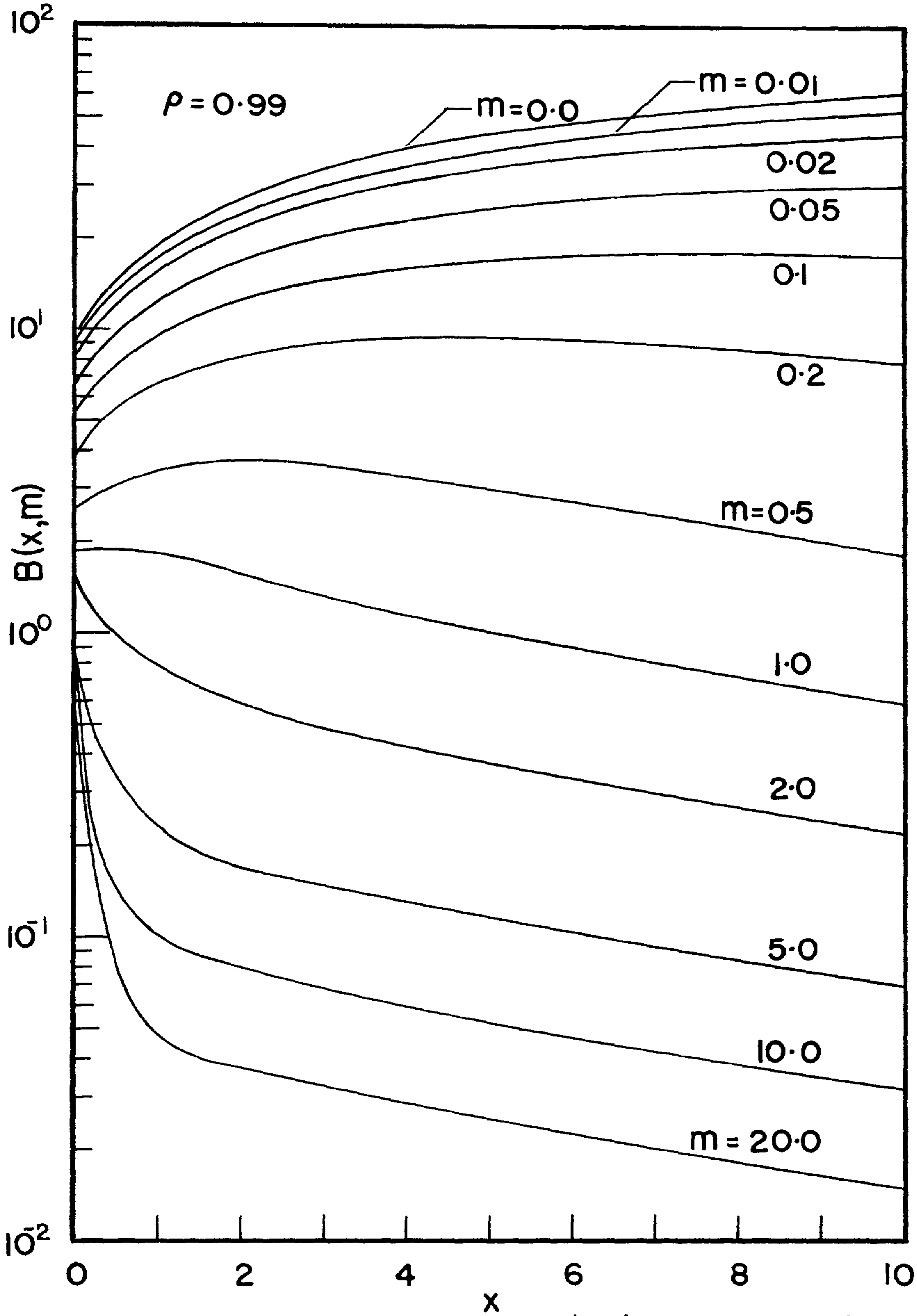

Figure 4.12 - Dimensionless radiosity B(x,m) variation within the cavity for ρ = 0.99

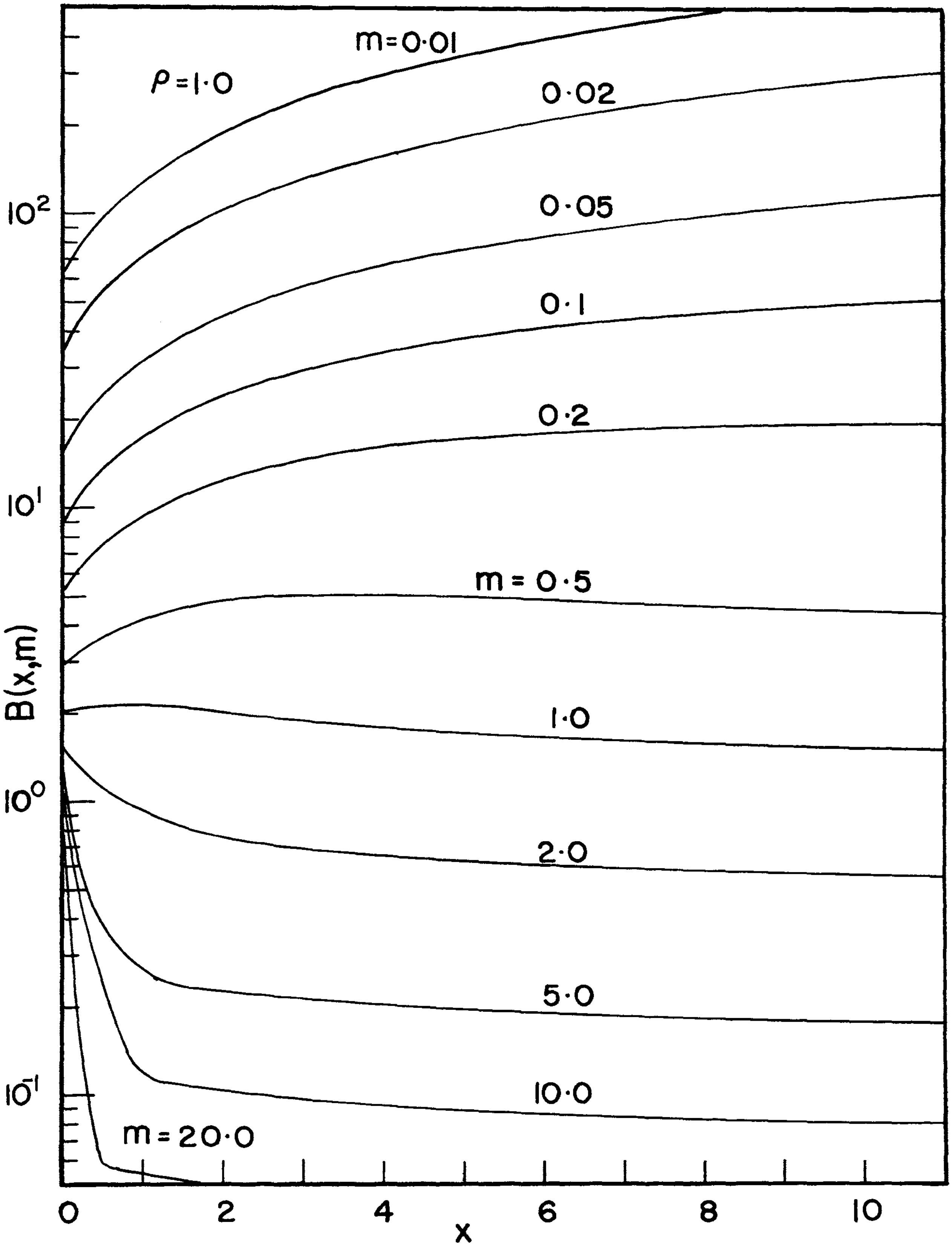

Figure 4.13 - Dimensionless radiosity B(x,m) variation within the cavity for ρ = 1.0

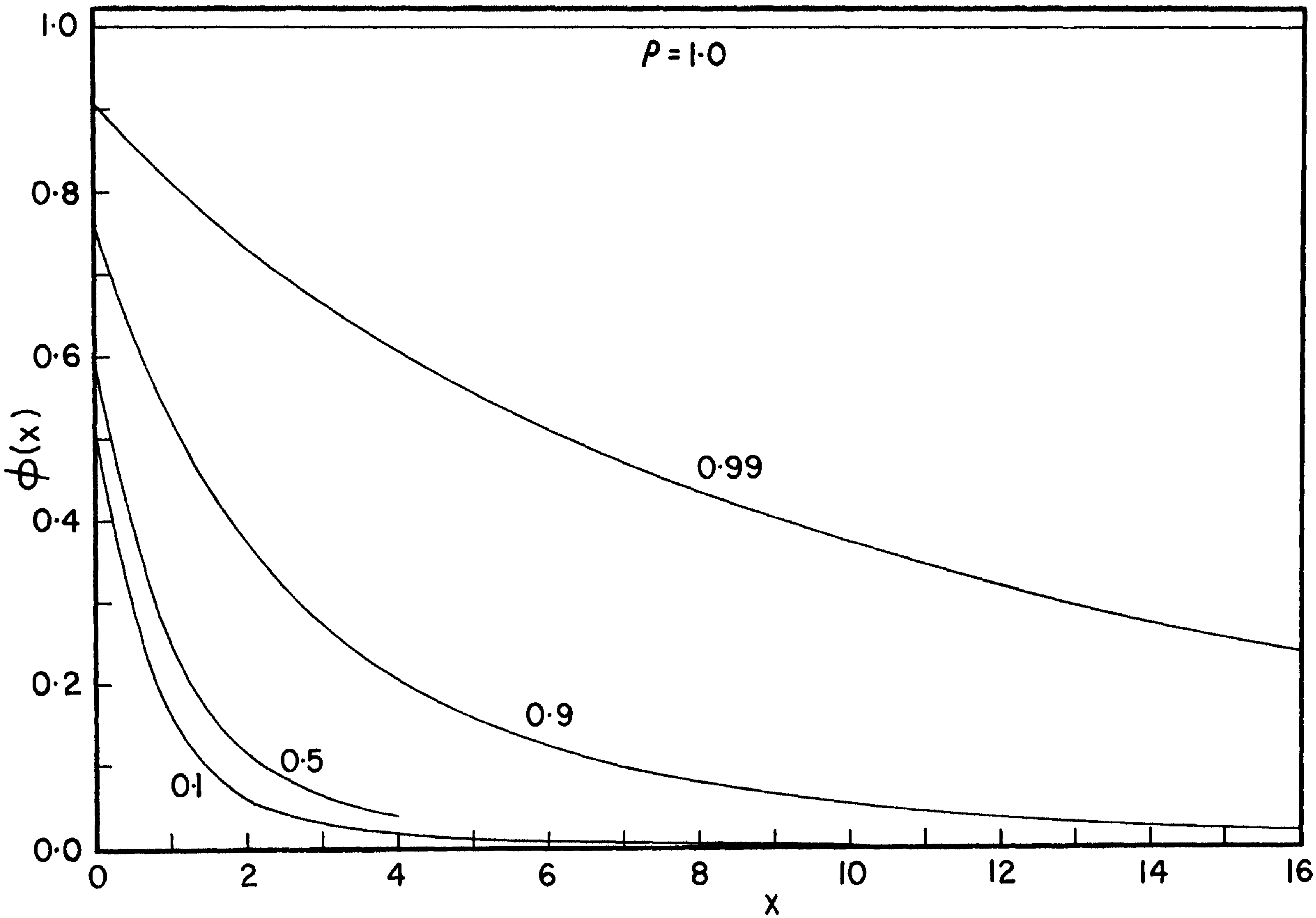

Figure 4.14 - Dimensionless radiosity $\phi(x)$ variation within the cavity

larger is the magnitude of the radiosity $\phi(x)$. The maximum dimensionless radiosity occurs at the edge of the cavity and is equal to $\frac{1}{2}\alpha_0$. At ρ = 0.1, 0.5, 0.9 and 0.99, $\phi(x)$ decreases with depth into the cavity. The trend of all the curves in Figure 4.14 is that for large x the radiosity $\phi(x)$ approaches zero.

For a uniform temperature distribution m = 0, values of the local apparent emittance [$\varepsilon_a = \varepsilon B(x,0)$] for ε = 0.9, 0.5, 0.1 and 0.01 are listed in Table 4.8. Also the local apparent emittance is presented graphically in Figure 4.15. Regardless the value of ρ, the local apparent emittance approaches the value of unity deep within the cavity. An apparent emittance of unity means that the surface pears to be a black body. Obviously, from the curves in Figure 4.15, the larger the value of emittance, ε, the faster the apparent emittance ε_a approaches unity.

C. LOCAL HEAT FLUX.

The values of local heat flux are calculated using equation (3-12)

$$q(x,m) = \frac{1}{\rho}\ e^{-mx} - \varepsilon B(x,m) \quad .$$

For m = 0 and 1.0, the values of local heat flux are listed in Tables 4.9 and 4.10 and presented graphically in Figures 4.16 and 4.17, respectively. In the case represented in Figure 4.16 the surfaces of the cavity are held at a uniform temperature. As seen, the larger the value of ρ the larger, the magnitude of the heat flux at the edge of the cavity. The magnitude of the local heat flux at the edge of the cavity for all ρ is larger for the m = 1.0 case. The curves in Figure

Table 4.8

Apparent emittance ε_a for isothermal cavity

x	ρ = 0.10	ρ = 0.50	ρ = 0.90	ρ = 0.99
0.0	0.94868	0.70710	0.31623	0.10000
0.01	0.94917	0.70923	0.31850	0.10094
0.05	0.95113	0.71775	0.32766	0.10474
0.10	0.95356	0.72840	0.33923	0.10957
0.20	0.95830	0.74947	0.36259	0.11943
0.30	0.96280	0.76983	0.38586	0.12942
0.40	0.96697	0.78910	0.40871	0.13941
0.50	0.97075	0.80703	0.43085	0.14930
0.60	0.97411	0.82350	0.45214	0.15903
0.70	0.97709	0.83850	0.47248	0.16856
0.80	0.97970	0.85208	0.49185	0.17787
0.90	0.98197	0.86432	0.51027	0.18696
1.00	0.98394	0.87535	0.52778	0.19582
1.50	0.99054	0.91620	0.60335	0.23718
2.00	0.99396	0.94126	0.66326	0.27449
2.50	0.99588	0.95735	0.71176	0.30865
3.00	0.99703	0.96811	0.75163	0.34023
4.00	0.99827	0.98083	0.81260	0.39715
5.00	0.99888		0.85612	0.44732
6.00	0.99922		0.88792	0.49203
7.00	0.99942		0.91157	0.53217
8.00	0.99956		0.92942	0.56840
10.00	0.99972		0.95360	0.63108
12.00			0.96831	0.68314
15.00			0.98093	0.74592
20.00			0.99054	0.80850

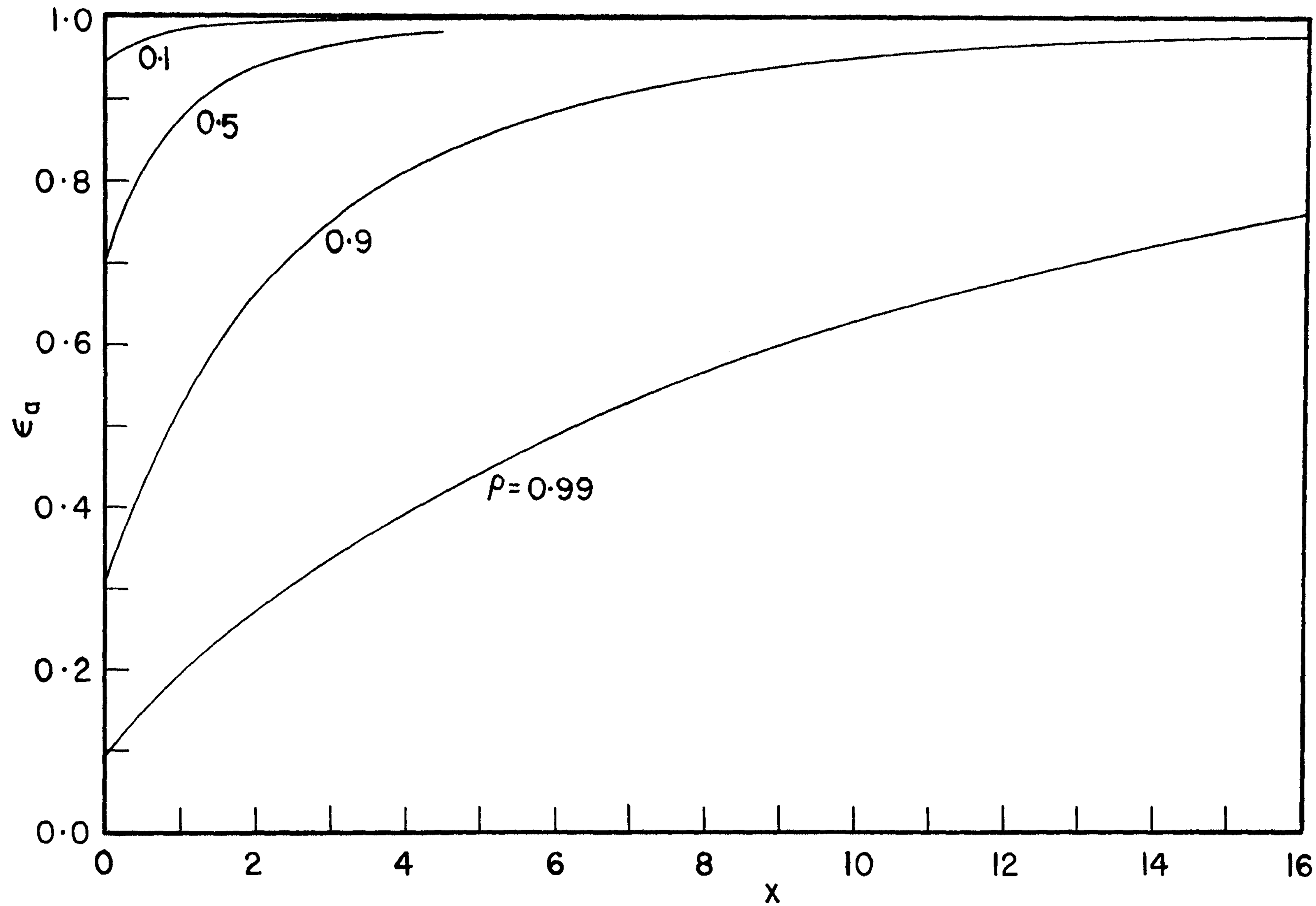

Figure 4.15 - Apparent emittance versus depth into the cavity

Table 4.9

Local heat flux q(x,m) for isothermal cavity

x	ρ = 0.10	ρ = 0.50	ρ = 0.90	ρ = 0.99
0.0	0.51317	0.58579	0.75975	0.90909
0.01	0.50828	0.58154	0.75722	0.90814
0.05	0.48873	0.56450	0.74705	0.90430
0.10	0.46444	0.54319	0.73419	0.89942
0.20	0.41696	0.50105	0.70824	0.88946
0.30	0.37196	0.46033	0.68237	0.87937
0.40	0.33031	0.42180	0.65699	0.86928
0.50	0.26253	0.38594	0.63238	0.85929
0.60	0.25880	0.35299	0.60873	0.84946
0.70	0.22903	0.32299	0.58613	0.83984
0.80	0.20298	0.29584	0.56460	0.83043
0.90	0.18029	0.27135	0.54414	0.82125
1.00	0.16059	0.24929	0.52469	0.81230
1.50	0.09460	0.16758	0.44072	0.77052
2.00	0.06041	0.11747	0.37416	0.73283
2.50	0.04125	0.08528	0.32027	0.69833
3.00	0.02968	0.06377	0.27597	0.66643
4.00	0.01726	0.03834	0.20822	0.60894
5.00	0.01118		0.15986	0.55826
6.00	0.00779		0.12454	0.51310
7.00	0.00572		0.09826	0.47255
8.00	0.00438		0.07843	0.43596
10.00	0.00279		0.05156	0.37264
12.00			0.03521	0.32005
15.00			0.02118	0.25665
20.00			0.01051	0.18056

Table 4.10

Local heat flux q(x,m) for m = 1.0

x	ρ = 0.10	ρ = 0.50	ρ = 0.90	ρ = 0.99
0.0	0.74410	0.81312	0.93665	0.99111
0.01	0.73195	0.80148	0.92608	0.98107
0.05	0.68456	0.75604	0.88481	0.94189
0.10	0.62805	0.70172	0.83543	0.89506
0.20	0.52422	0.60129	0.74367	0.80810
0.30	0.43258	0.51157	0.66068	0.72940
0.40	0.35277	0.43213	0.58582	0.65818
0.50	0.28415	0.36239	0.51844	0.59376
0.60	0.22582	0.30161	0.45794	0.53549
0.70	0.17673	0.24896	0.40368	0.48281
0.80	0.13575	0.20361	0.35510	0.43519
0.90	0.10179	0.16469	0.31164	0.39213
1.00	0.07383	0.13141	0.27280	0.35321
1.50	0.00044	0.02687	0.13298	0.20808
2.00	-0.02829	-0.01616	0.05488	0.12065
2.50	-0.03155	-0.03069	0.01241	0.06809
3.00	-0.02784	-0.03260	-0.00965	0.03659
4.00	-0.01742	-0.02475	-0.02421	0.00670
5.00	-0.00997		-0.02368	-0.00350
6.00	-0.00567		-0.01953	-0.00661
7.00	-0.00331		-0.01524	-0.00721
8.00	-0.00202		-0.01169	-0.00696
10.00	-0.00087		-0.00689	-0.00594
12.00			-0.00418	-0.00496
15.00			-0.00211	-0.00381
20.00			-0.00079	-0.00253

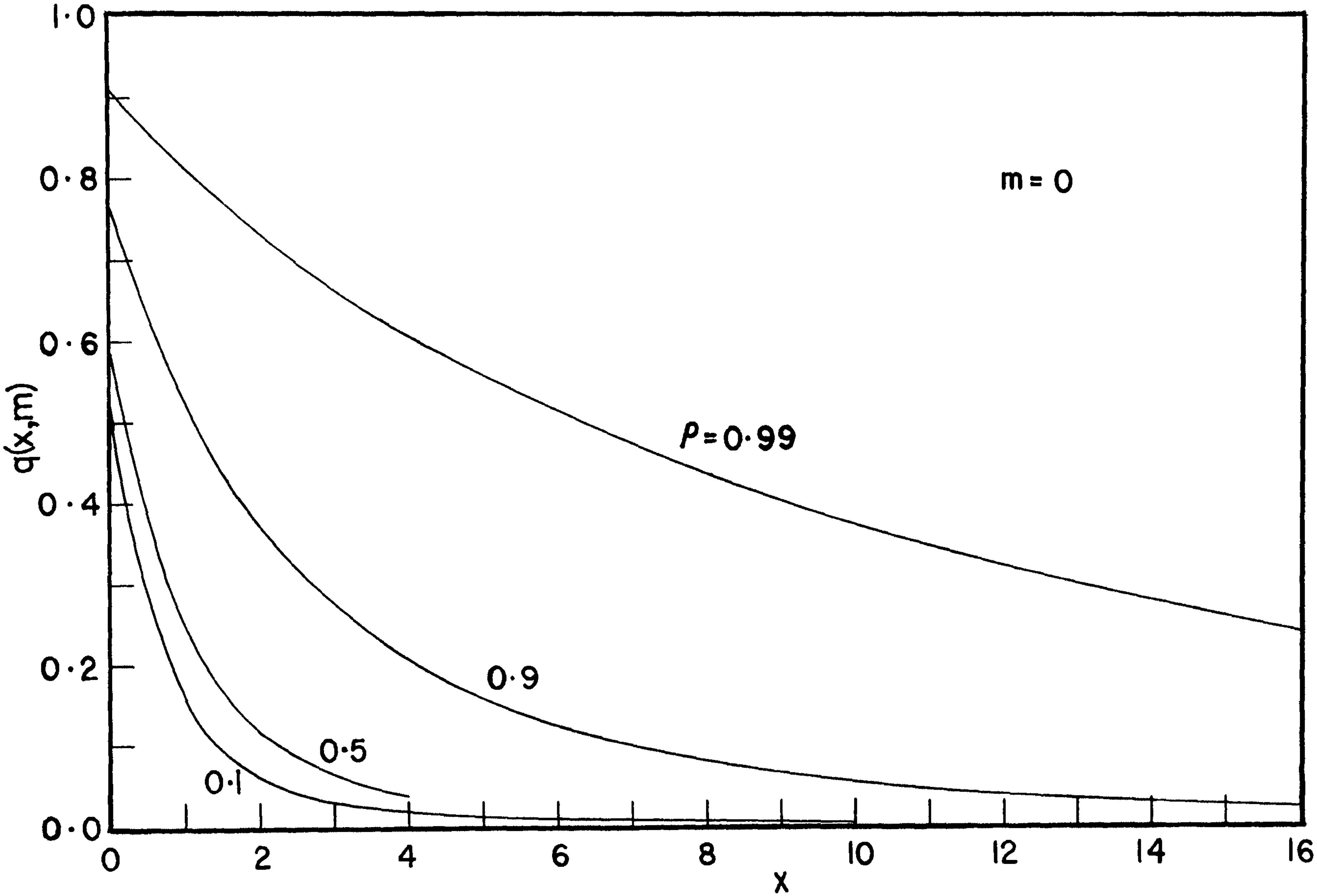

Figure 4.16 - Local heat flux for an isothermal rectangular cavity

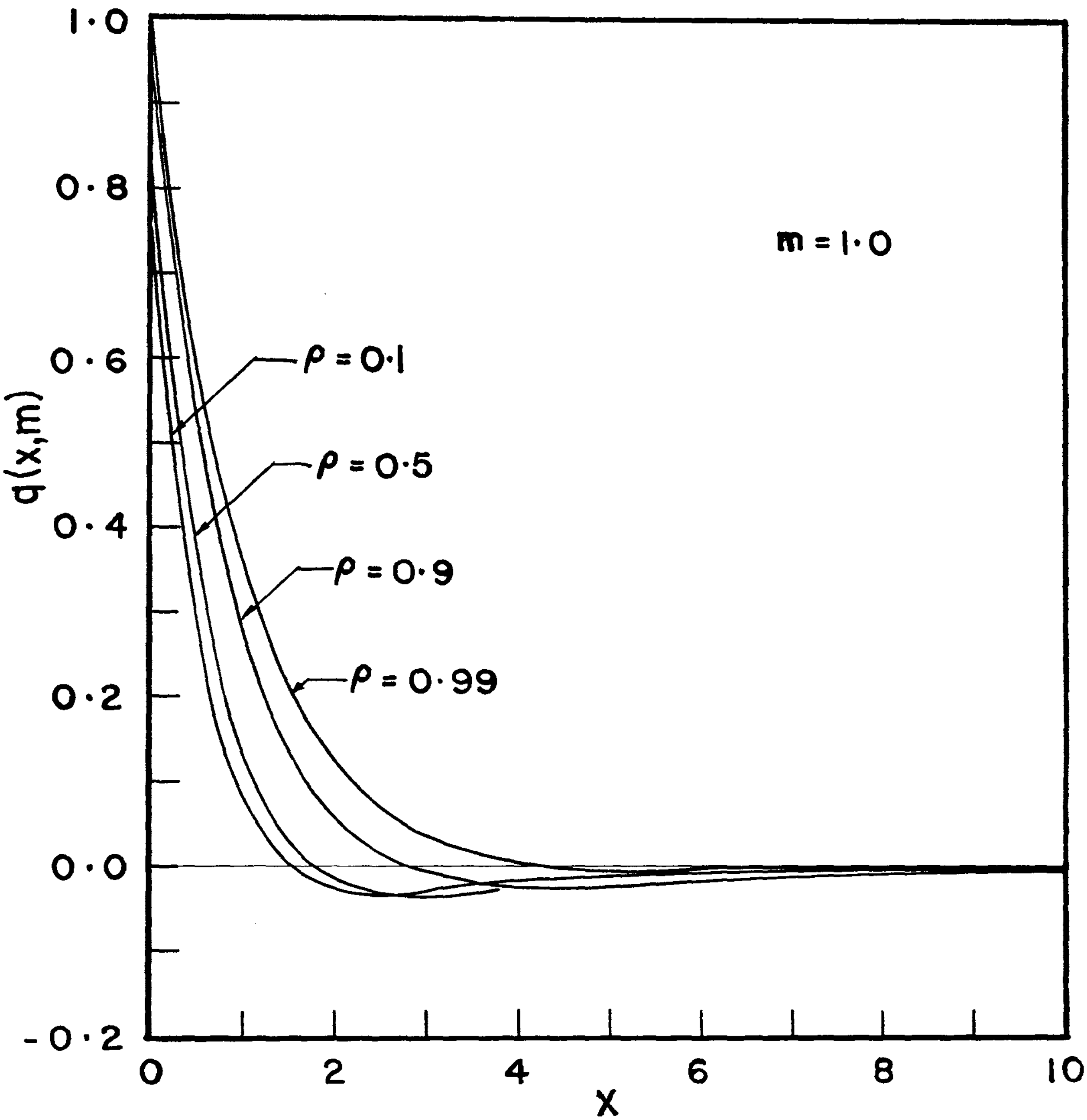

Figure 4.17 - Local heat flux for m = 1.0

4.17 have steeper slopes when compared with the curves in Figure 4.16. Notice in Figure 4.17 the curves dip below zero and then converge to zero. The negative value means that the flux incident on the surface is greater than the flux leaving the surface. The emission at the location where the negative heat flux occurs is low regardless the emittance because the temperature is low. Also if the reflectance ρ of the surface is large, most of the heat flux incident on the location would be reflected back. Consequently, the smaller the value of ρ the larger the magnitude of negative heat flux.

Figure 4.18 exhibits the variance in local heat flux $q(x,m)$ with depth into the cavity for $\rho = 0.9$. The curves correspond to $m = 0$, 0.1, 1.0 and 10.0. These values are presented in Table 4.11. As the temperature distribution parameter m increases the local heat flux at the edge of the cavity increases and the decay of the heat flux with depth increases. All the curves seem to converge to zero but at various depths into the cavity and the slopes of the curves decrease with the increase in the value of m.

D. HEAT TRANSFER.

The overall heat transfer of the cavity is determined by equations of the form

$$Q(m) = \frac{1 - H(m)\sqrt{\varepsilon}}{\rho m}$$

and

$$Q(0) = \frac{\alpha_1}{2\sqrt{\varepsilon}}$$

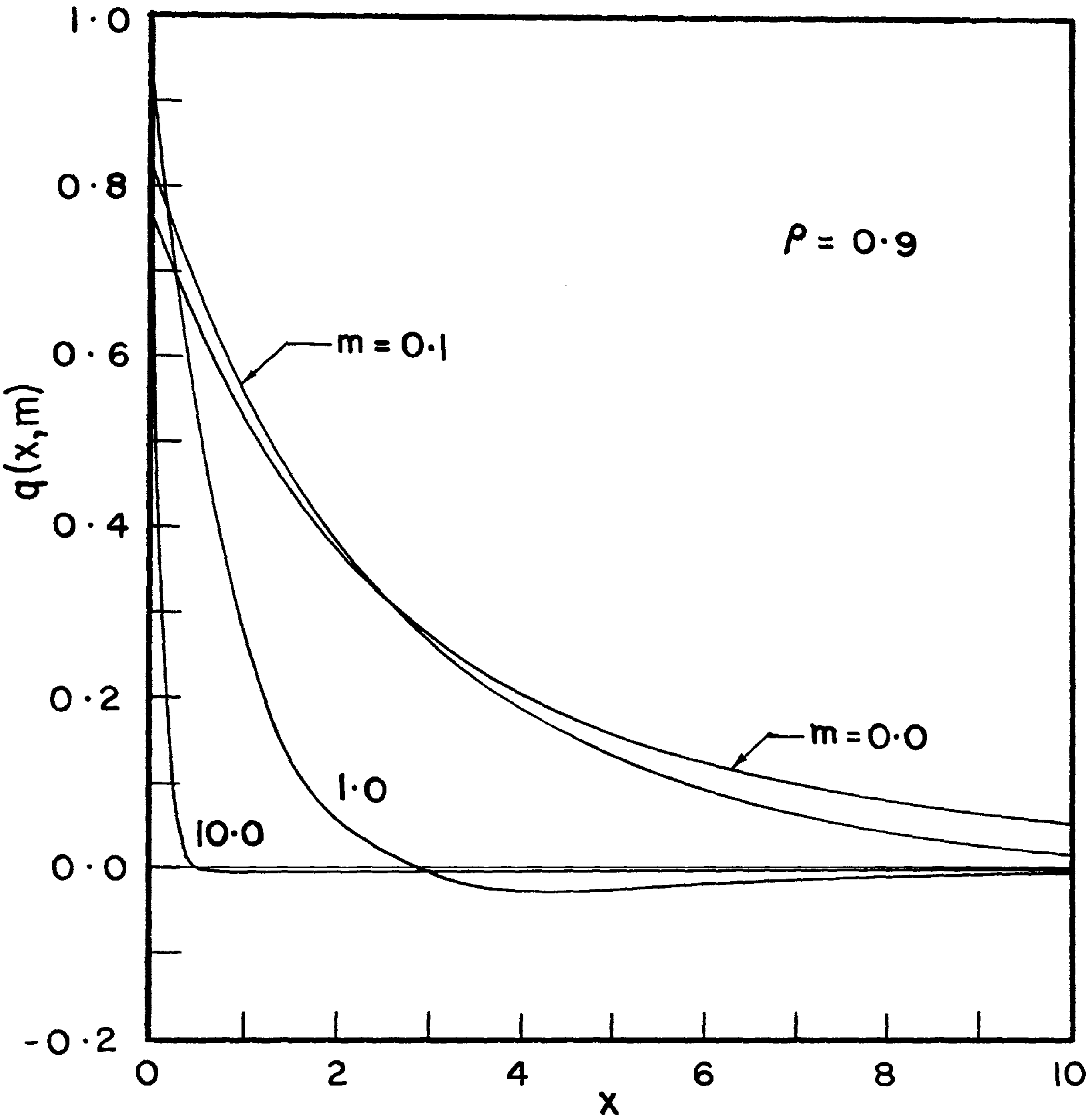

Figure 4.18 - Local heat flux for ρ = 0.9

Table 4.11

Local heat flux q(x,m) for ρ = 0.9

x	m = 0.00	m = 0.10	m = 1.00	m = 10.00
0.0	0.75975	0.81770	0.93665	0.99190
0.01	0.75722	0.81478	0.92608	0.89669
0.05	0.74705	0.80305	0.88481	0.59822
0.10	0.73419	0.78833	0.83543	0.35941
0.20	0.70824	0.75892	0.74367	0.12664
0.30	0.68237	0.72988	0.66068	0.04104
0.40	0.65699	0.70153	0.58582	0.00966
0.50	0.63238	0.67411	0.51844	-0.00171
0.60	0.60873	0.64775	0.45794	-0.00568
0.70	0.58613	0.62252	0.40368	-0.00692
0.80	0.56460	0.59844	0.35510	-0.00714
0.90	0.54414	0.57548	0.31164	-0.00700
1.00	0.52469	0.55360	0.27280	-0.00673
2.00	0.37416	0.38176	0.05488	-0.00380
3.00	0.27597	0.26765	-0.00965	-0.00284
4.00	0.20822	0.18850	-0.02421	-0.00199
5.00	0.15986	0.13224	-0.02368	-0.00144
6.00	0.12454	0.09165	-0.01953	-0.00106
7.00	0.09826	0.06210	-0.01524	-0.00079
8.00	0.07843	0.04047	-0.01169	-0.00060
9.00	0.06327	0.02460	-0.00909	-0.00046
10.00	0.05156	0.01297	-0.00689	-0.00036
11.00	0.04241	0.00448	-0.00535	-0.00028
12.00	0.03521	-0.00165	-0.00418	-0.00022
13.00	0.02948	-0.00604	-0.00330	-0.00018
14.00	0.02489	-0.00911	-0.00263	-0.00014
15.00	0.02118	-0.01118	-0.00211	-0.00011
16.00	0.01816	-0.01251	-0.00171	-0.00009
17.00	0.01568	-0.01329	-0.00139	-0.00008
18.00	0.01364	-0.01365	-0.00114	-0.00006
19.00	0.01193	-0.01370	-0.00095	-0.00005
20.00	0.01051	-0.01353	-0.00079	-0.00004

The values of heat transfer $Q(m)$ for various values of m have been computed for ρ = 0.1, 0.5, 0.9, 0.99 and 1.0 and are presented in Table 4.12 as well as in Figure 4.19. The general trends of the curves are as follows:

1. Small changes in ρ from unity cause large changes in $Q(m)$ when m is small. For large m the changes are small,
2. The dimensionless heat transfer $Q(m)$ increases as the reflectance ρ of the surfaces of the cavity is increased,
3. The larger the value of m, the lower the value of heat transfer $Q(m)$,
4. The maximum heat transfer occurs when the surfaces are held at uniform temperature, i.e., $m = 0$. For very large value of m the dimensionless heat transfer approaches zero.

The values of overall apparent emittance $[\bar{\varepsilon}_a = 2\varepsilon Q(m)/\sigma T_r^4]$ of the cavity are listed in Table 4.13. For isothermal surfaces and ρ = 0.5 and 0.1 the values of $\bar{\varepsilon}_a$ are in agreement with those of Sparrow [21, p. 167].

Table 4.12

Heat transfer Q(m)

m	ρ = 0.10	ρ = 0.50	ρ = 0.90	ρ = 0.99	ρ = 1.00
0.000	0.54299	0.85198	2.69514	11.8172	∞
0.001	0.53651	0.84791	2.67482	11.5788	1000.00
0.005	0.53421	0.83652	2.60675	10.8007	200.000
0.010	0.52700	0.82428	2.53624	10.0340	100.000
0.020	0.51729	0.80345	2.41743	8.85257	50.0000
0.030	0.50804	0.78543	2.31611	7.95354	33.0000
0.040	0.49961	0.76917	2.22663	7.23579	25.0000
0.050	0.49190	0.75424	2.14618	6.64563	20.0000
0.060	0.48455	0.74038	2.07300	6.14997	16.6667
0.070	0.47767	0.72738	2.00587	5.72681	14.2857
0.080	0.47132	0.71512	1.94389	5.36074	12.5000
0.090	0.46512	0.70350	1.88636	5.04056	11.1111
0.100	0.45931	0.69246	1.83274	4.75790	10.0000
0.200	0.41147	0.60387	1.43977	3.06854	5.00000
0.300	0.37570	0.53971	1.19434	2.27523	3.33333
0.400	0.34702	0.48976	1.02375	1.81126	2.50000
0.500	0.32313	0.44926	0.89739	1.50591	2.00000
0.600	0.30278	0.41552	0.79966	1.28937	1.66667
0.700	0.28511	0.38686	0.72164	1.12766	1.42857
0.800	0.26959	0.36214	0.65780	1.00223	1.25000
0.900	0.25579	0.34055	0.60454	0.90205	1.11111
1.000	0.24343	0.32150	0.55941	0.82017	1.00000
2.000	0.16522	0.20741	0.32152	0.43064	0.50000
3.000	0.12539	0.15347	0.22598	0.29219	0.33333
4.000	0.10105	0.12183	0.17426	0.22114	0.25000
5.000	0.08460	0.10099	0.14181	0.17788	0.20000
6.000	0.07273	0.08623	0.11955	0.14878	0.16666
7.000	0.06377	0.07522	0.10332	0.12787	0.14286
8.000	0.05677	0.06670	0.09096	0.11210	0.12500
9.000	0.05115	0.05991	0.08125	0.09980	0.11111
10.000	0.04654	0.05437	0.07341	0.08993	0.10000
15.000	0.03206	0.03717	0.04951	0.06028	0.06667
20.000	0.02444	0.02823	0.03735	0.04521	0.05000
25.000	0.01975	0.02275	0.02998	0.03621	0.04000
30.000	0.01656	0.01905	0.02504	0.03020	0.03333
35.000	0.01426	0.01639	0.02150	0.02589	0.02857
40.000	0.01252	0.01438	0.01883	0.02267	0.02500
45.000	0.01116	0.01281	0.01676	0.02015	0.02222
50.000	0.01007	0.01154	0.01509	0.01814	0.02000
100.000	0.00508	0.00581	0.00757	0.00908	0.01000
200.000	0.00255	0.00292	0.00379	0.00454	0.00500
300.000	0.00170	0.00195	0.00253	0.00303	0.00333
400.000	0.00128	0.00146	0.00190	0.00227	0.00250
500.000	0.00102	0.00117	0.00152	0.00182	0.00200
1000.000	0.00051	0.00058	0.00076	0.00090	0.00100

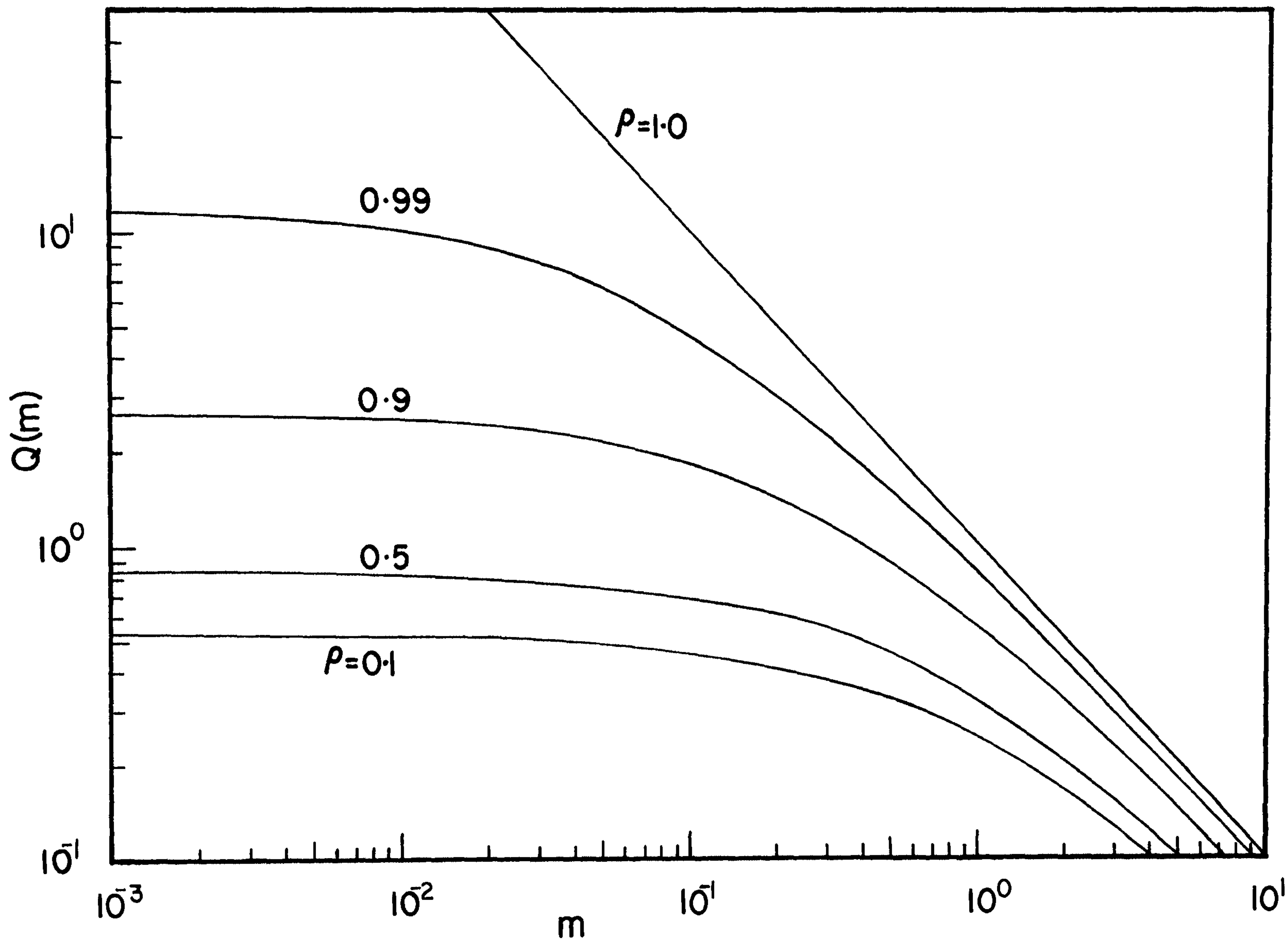

Figure 4.19 - Heat transfer Q(m) versus m

Table 4.13

Overall emittance $\overline{\varepsilon}_a$

m	ρ = 0.10	ρ = 0.50	ρ = 0.90	ρ = 0.99
0.000	0.97738	0.85198	0.53903	0.23634
0.001	0.96572	0.84791	0.53496	0.23157
0.005	0.96158	0.83652	0.52135	0.21601
0.010	0.95039	0.82428	0.50725	0.20068
0.020	0.93113	0.80345	0.48349	0.17705
0.030	0.91447	0.78543	0.46322	0.15907
0.040	0.89930	0.76917	0.44532	0.14471
0.050	0.88542	0.75424	0.42923	0.13291
0.060	0.87219	0.74038	0.41460	0.12300
0.070	0.85980	0.72738	0.40117	0.11454
0.080	0.84838	0.71512	0.38878	0.10721
0.090	0.83722	0.70350	0.37727	0.10081
0.100	0.82676	0.69246	0.36655	0.09516
0.200	0.74065	0.60387	0.28795	0.06137
0.300	0.67625	0.53971	0.23887	0.04550
0.400	0.62463	0.48976	0.20475	0.03622
0.500	0.58164	0.44926	0.17948	0.03012
0.600	0.54500	0.41552	0.15993	0.02579
0.700	0.51320	0.38686	0.14433	0.02255
0.800	0.48526	0.36214	0.13156	0.02004
0.900	0.46042	0.34055	0.12091	0.01804
1.000	0.43817	0.32150	0.11188	0.016403
2.000	0.29740	0.20741	0.06430	0.008612
3.000	0.22571	0.15347	0.04520	0.005843
4.000	0.18189	0.12183	0.03485	0.004422
5.000	0.15227	0.10099	0.02836	0.003557
6.000	0.13092	0.08623	0.02391	0.002975
7.000	0.11480	0.07522	0.02066	0.002557
8.000	0.10220	0.06670	0.01819	0.002242
9.000	0.09208	0.05991	0.01625	0.001996
10.000	0.08377	0.05437	0.01468	0.001898
15.000	0.05771	0.03717	0.009902	0.001203
20.000	0.04400	0.02823	0.007469	0.000904
25.000	0.03554	0.02275	0.005996	0.000724
30.000	0.02981	0.01905	0.005008	0.000603
35.000	0.02567	0.01639	0.004229	0.000517
40.000	0.02254	0.01438	0.003767	0.000453
45.000	0.02009	0.01281	0.003351	0.000403
50.000	0.01812	0.01154	0.003018	0.000362
100.000	0.00915	0.00581	0.001514	0.000181
200.000	0.00460	0.00292	0.000758	0.000090
300.000	0.00307	0.00195	0.000505	0.000060
400.000	0.00230	0.00146	0.000379	0.000045
500.000	0.00184	0.00117	0.000303	0.000036
1000.000	0.00092	0.00058	0.000151	0.000018

V. CONCLUSIONS AND RECOMMENDATIONS

Radiant interchange in a non-isothermal rectangular cavity has been investigated in the course of this work. The surfaces of the cavity have been considered to be gray diffuse with non-uniform radiosity. Application of Ambarzumian's method has yielded closed-form relations for the radiosity, heat transfer and apparent emittance of the cavity in terms of universal functions. This is the first time this approach has been used to determine the radiative heat transfer between surfaces. The investigation is made in such a way as to include many different thermal boundary conditions.

Some specific conclusions are summarized as follows:

1. The values of radiosity at the edge of the cavity and the overall heat transfer are found without determining the radiosity inside the cavity. The H-function for the isothermal cavity has the value equal to $1/\sqrt{\varepsilon}$.
2. Small changes in ρ from unity cause enormous change in the value of the H-function for small m whereas for large m the H-function approaches unity for all ρ.
3. The H-function, radiosity and heat transfer are maximum for an isothermal cavity.
4. Deep within the cavity little heat transfer between the surfaces takes place and the cavity appears to be a black body.
5. When the cavity is non-isothermal, negative heat fluxes occur. The smaller the value of ρ the larger the magnitude of the negative heat flux.

A number of radiative transfer problems have evolved during the course of this investigation. Some worthy of further study are listed below:

1. Radiant interchange between non-isothermal surfaces with other one-dimensional geometries.
2. Non-gray surfaces.
3. Surfaces with directional properties.
4. Two-dimensional geometries.

BIBLIOGRAPHY

1. H. Buckley, On the Radiation from the Inside of a Circular Cylinder, Phil. Mag. 4, 753-762 (1927).

2. H. Buckley, On the Radiation from the Inside of a Circular Cylinder - Part II, Phil. Mag. 6, 447-457 (1928).

3. E.R.G. Eckert and Robert M. Drake, Jr., Heat and Mass Transfer, McGraw-Hill Book Company, Inc. (1959).

4. Moon, P., Scientific Basis of Illumination Engineering, Dover Publications Inc., New York (1961).

5. E.M. Sparrow and L.U. Albers, Apparent Emissivity and Heat Transfer in a Long Cylindrical Hole, J. Heat Transfer 82, 253-255 (1960).

6. E.M. Sparrow, Application of Variational Methods to Radiation Heat-Transfer Calculations, J. Heat Transfer 82, 375-380 (1960).

7. C.M. Usisken and R. Seigel, Thermal Radiation from a Cylindrical Enclosure With Specified Wall Heat Flux, J. Heat Transfer 82, 369-374 (1960).

8. E.M. Sparrow, J.L. Gregg, J.V. Szel, and P. Manos, Analysis, Results, and Interpretation for Radiation Between Some Simply-Arranged Gray Surfaces, J. Heat Transfer 83, 207-214 (1961).

9. E.M. Sparrow and J.L. Gregg, Radiant Interchange Between Circular Disks Having Arbitrarily Different Temperatures, J. Heat Transfer 83, 494-500 (1961).

10. E.M. Sparrow and V.K. Jonsson, Absorption and Emission Characteristics of Diffuse Spherical Enclosures, NASA TN D - 1289 (1962).

11. E.M. Sparrow and V.K. Jonsson, The Transport of Radiant Energy Through Tapered Tubes or Tapered Gaps, J. Heat Transfer 86, 132 (1964).

12. E.M. Sparrow and A. Haji-Sheikh, A Generalized Variational Method for Calculating Radiant Interchange Between Surfaces, J. Heat Transfer 87, 103-109 (1965).

13. T.J. Love and J.S. Gilbert, Experimental Study of Radiative Heat Transfer Between Parallel Plates, ARL 66 - 0103 (1966).

14. P. Campanaro and T. Ricolfi, New Determination of the Total Normal Emissivity of Cylindrical and Conical Cavities, J. Optical Society of America 57 (1967).

15. A.L. Crosbie and R. Viskanta, Application of Sokolv's Method to Integral Equations of Radiant Interchange, Journal of Spacecraft and Rockets 4, 947-948 (1967).

16. T.J. Love and W.D. Turner, Higher Order Approximation for Lumped System Analysis of Evacuated Enclosures, AIAA 3rd Thermodynamics Conference, No. 68-768 (1968).

17. J.S. Toor, R. Viskanta and E.R.F. Winter, Radiant Heat Transfer Between Simply Arranged Surfaces with Direction Dependent Properties, AIAA Paper No. 69-624 (1969).

18. M.L. Rasmussen and M.C. Jischke, Radiant Heat Transfer at the Vertex of Adjoint Plates, AIAA Journal 8, 1360-1361 (1970).

19. D.C. Look and T.J. Love, Numerical Quadrature and Radiative Heat Transfer Computations, AIAA Journal 8, 819-820 (1970).

20. E.M. Sparrow and A. Haji-Sheikh, The Solution of Radiative Exchange Problems by Least Squares Techniques, Int. J. Heat Mass Transfer 13, 647-650 (1970).

21. E.M. Sparrow and R.D. Cess, Radiative Heat Transfer, Brooks/Cole Publishing Company, Belmont, California (1970).

22. T.J. Love, Radiative Heat Transfer, Merril Publishing Company, Columbus, Ohio (1968).

23. V. Kourganoff, Basic Methods in Transfer Problems, Oxford University Press, London (1952).

24. I.M. Longman, Note on a Method for Computing Infinite Integrals of Oscillatory Functions, Camb. Philos. 52, 764-768 (1956).

25. Robert L. Ketter and Sherwood P. Prawel, Jr., Modern Methods of Engineering Computation, McGraw-Hill Book Company (1969).

VITA

Tilak Raj Sawheny was born on November 1, 1946, in Lahore, India. He got his primary and high school education in Lndhiana, India. He received Diploma in Mechanical Engineering from State Board of Technical Education, Chandigarh, India, in October 1966.

He came to U.S.A. as an undergraduate student in the University of Michigan in spring of 1967. He worked with Professor J. Datsko as research assistant for about two years. He was assistant to a research engineer in Kelsey Hayes Company Research and Development Center in summer of 1969. He graduated in December 1969 receiving his Bachelor's degree in Mechanical Engineering from the University of Michigan.

He has been enrolled in Graduate School of the University of Missouri-Rolla since January 1970.